California State Waters Map Series—Offshore of Salt Point, California

By Samuel Y. Johnson, Peter Dartnell, Nadine E. Golden, Stephen R. Hartwell, Mercedes D. Erdey, H. Gary Greene, Guy R. Cochrane, Rikk G. Kvitek, Michael W. Manson, Charles A. Endris, Bryan E. Dieter, Janet T. Watt, Lisa M. Krigsman, Ray W. Sliter, Erik N. Lowe, and John L. Chin

(Samuel Y. Johnson and Susan A. Cochran, editors)

Pamphlet to accompany

Open-File Report 2015–1098

2015

U.S. Department of the Interior
U.S. Geological Survey

U.S. Department of the Interior
SALLY JEWELL, Secretary
U.S. Geological Survey
Suzette M. Kimball, Acting Director

U.S. Geological Survey, Reston, Virginia: 2015

Suggested citation:
Johnson, S.Y., Dartnell, P., Golden, N.E., Hartwell, S.R., Erdey, M.D., Greene, H.G., Cochrane, G.R., Kvitek, R.G., Manson, M.W., Endris, C.A., Dieter, B.E., Watt, J.T., Krigsman, L.M., Sliter, R.W., Lowe, E.N., and Chin, J.L. (S.Y. Johnson and S.A. Cochran, eds.), 2015, California State Waters Map Series—Offshore of Salt Point, California: U.S. Geological Survey Open-File Report 2015–1098, pamphlet 37 p., 10 sheets, scale 1:24,000, http://dx.doi.org/10.3133/ofr20151098.

ISSN 2331-1258 (online)

Contents

Figures

Tables

Map Sheets

California State Waters Map Series—Offshore of Salt Point, California

By Samuel Y. Johnson,[1] Peter Dartnell,[1] Nadine E. Golden,[1] Stephen R. Hartwell,[1] Mercedes D. Erdey,[1] H. Gary Greene,[2] Guy R. Cochrane,[1] Rikk G. Kvitek,[3] Michael W. Manson,[4] Charles A. Endris,[2] Bryan E. Dieter,[2] Janet T. Watt,[1] Lisa M. Krigsman,[5] Ray W. Sliter,[1] Erik N. Lowe,[1] and John L. Chin[1]

(Samuel Y. Johnson[1] and Susan A. Cochran,[1] editors)

Preface

In 2007, the California Ocean Protection Council initiated the California Seafloor Mapping Program (CSMP), designed to create a comprehensive seafloor map of high-resolution bathymetry, marine benthic habitats, and geology within California's State Waters. The program supports a large number of coastal-zone- and ocean-management issues, including the California Marine Life Protection Act (MLPA) (California Department of Fish and Wildlife, 2008), which requires information about the distribution of ecosystems as part of the design and proposal process for the establishment of Marine Protected Areas. A focus of CSMP is to map California's State Waters with consistent methods at a consistent scale.

The CSMP approach is to create highly detailed seafloor maps through collection, integration, interpretation, and visualization of swath sonar data (the undersea equivalent of satellite remote-sensing data in terrestrial mapping), acoustic backscatter, seafloor video, seafloor photography, high-resolution seismic-reflection profiles, and bottom-sediment sampling data. The map products display seafloor morphology and character, identify potential marine benthic habitats, and illustrate both the surficial seafloor geology and shallow (to about 100 m) subsurface geology. It is emphasized that the more interpretive habitat and geology maps rely on the integration of multiple, new high-resolution datasets and that mapping at small scales would not be possible without such data.

This approach and CSMP planning is based in part on recommendations of the Marine Mapping Planning Workshop (Kvitek and others, 2006), attended by coastal and marine managers and scientists from around the state. That workshop established geographic priorities for a coastal mapping project and identified the need for coverage of "lands" from the shore strand line (defined as Mean Higher High Water; MHHW) out to the 3-nautical-mile (5.6-km) limit of California's State Waters. Unfortunately, surveying the zone from MHHW out to 10-m water depth is not consistently possible using ship-based surveying methods, owing to sea state (for example, waves, wind, or currents), kelp coverage, and shallow rock outcrops. Accordingly, some of the maps presented in this series commonly do not cover the zone from the shore out to 10-m depth; these "no data" zones appear pale gray on most maps.

This map is part of a series of online U.S. Geological Survey (USGS) publications, each of which includes several map sheets, some explanatory text, and a descriptive pamphlet. Each map sheet

[1] U.S. Geological Survey
[2] Moss Landing Marine Laboratories, Center for Habitat Studies
[3] California State University Monterey Bay, Seafloor Mapping Lab
[4] California Geological Survey
[5] National Oceanic and Atmospheric Administration, National Marine Fisheries Service

is published as a PDF file. Geographic information system (GIS) files that contain both ESRI[6] ArcGIS raster grids (for example, bathymetry, seafloor character) and geotiffs (for example, shaded relief) are also included for each publication. For those who do not own the full suite of ESRI GIS and mapping software, the data can be read using ESRI ArcReader, a free viewer that is available at http://www.esri.com/software/arcgis/arcreader/index.html (last accessed February 5, 2014).

The California Seafloor Mapping Program (CSMP) is a collaborative venture between numerous different federal and state agencies, academia, and the private sector. CSMP partners include the California Coastal Conservancy, the California Ocean Protection Council, the California Department of Fish and Wildlife, the California Geological Survey, California State University at Monterey Bay's Seafloor Mapping Lab, Moss Landing Marine Laboratories Center for Habitat Studies, Fugro Pelagos, Pacific Gas and Electric Company, National Oceanic and Atmospheric Administration (NOAA, including National Ocean Service—Office of Coast Surveys, National Marine Sanctuaries, and National Marine Fisheries Service), U.S. Army Corps of Engineers, the Bureau of Ocean Energy Management, the National Park Service, and the U.S. Geological Survey.

[6] Environmental Systems Research Institute, Inc.

Chapter 1. Introduction

By Samuel Y. Johnson

Regional Setting

The map area offshore of Salt Point, California, which is referred to herein as the "Offshore of Salt Point" map area (figs. 1–1, 1–2), is located in northern California, about 110 km north of San Francisco and 50 km south of Point Arena. The map area includes three California Marine Protected Areas (MPA; California Department of Fish and Wildlife, 2012): the southern portion of the Stewarts Point State Marine Reserve, the Salt Point State Marine Conservation Area, and the Gerstle Cove State Marine Reserve (fig. 1–2). The coast and shoreline are rugged and scenic, characterized by rocky promontories, steep bluffs capped by bare to forested marine terraces, kelp-rich coves, and nearshore rocks and pinnacles. The largely undeveloped onshore part of the map area is used primarily for grazing and recreation. U.S. Highway 1 extends along the coast through the map area, passing through Salt Point State Park, Kruse Rhododendron State Natural Reserve, and Stillwater Cove Regional Park (fig. 1–2). Although coastal watersheds are steep, they extend to a drainage divide just 2 to 3 km east of the shoreline and local sediment supply to the coast is limited. Sandy beaches are uncommon, present only in relatively protected coves.

The seafloor in the map area extends from the shoreline to water depths of about 90 to 100 m. The nearshore to inner shelf area (to water depths of about 50 to 60 m) typically dips seaward about 1.0° to 1.5° and is underlain by bedrock and sand-sized to coarser grained sediment. The midshelf, underlain predominantly by muddy sediments, slopes more gently (less than 0.5°). Surficial and shallow sediments were deposited in the last about 21,000 years during the approximately 125-m sea-level rise that followed the last major lowstand associated with the Last Glacial Maximum (Fairbanks, 1989; Fleming and others, 1998; Lambeck and Chappell, 2001; Peltier and Fairbanks, 2006), at which time the entire Offshore of Salt Point map area was emergent and the shoreline was about 20 km west of the present-day shoreline.

Circulation over the continental shelf in the map area (and in the broader northern California region) is dominated by the southward-flowing California Current, the eastern limb of the North Pacific Gyre (Hickey, 1979). Associated upwelling brings cool, nutrient-rich waters to the surface, resulting in high biological productivity. The current flow generally is southeastward during the spring and summer; however, during the fall and winter, the otherwise persistent northwest winds are sometimes weak or absent, causing the California Current to move farther offshore and the Davidson Current, a weaker, northward-flowing countercurrent (Hickey, 1979), to become active.

Throughout the year, this part of the central California coast is exposed to four wave climate regimes: the north Pacific swell, the southern swell, northwest wind waves, and local wind waves (Storlazzi and Griggs, 2000; Storlazzi and Wingfield, 2005). The north Pacific swell dominates in winter months (typically November through March), with wave heights at offshore buoys ranging from 2 to 10 m and wave periods ranging from 10 to 25 s (Storlazzi and Wingfield, 2005). During summer months, the largest waves come from the southern swell, generated by storms in the south Pacific and offshore Central America. Characteristically, these swells have smaller wave heights (0.3 to 3 m) and similarly long periods (range 10 to 25 s). Northwest wind waves affect the coast throughout the year, while local wind waves are most common from October to April. These two wind-wave regimes typically have wave heights of 1 to 4 m and short periods (3 to 10 s).

Potential marine benthic habitats in the Offshore of Salt Point map area include unconsolidated continental-shelf sediments, mixed continental-shelf substrate, and hard continental-shelf substrate. Rocky-shelf outcrops and rubble are considered to be promising potential habitats for rockfish and lingcod (Cass and others, 1990; Love and others, 2002), both of which are recreationally and commercially important species.

The onshore part of the Offshore of Salt Point map area is cut by the northwest-striking San Andreas Fault—the right-lateral transform boundary between the North American and Pacific tectonic plates. The San Andreas Fault extends offshore about 5 km south of the map area near Fort Ross, and about 50 km north of the map area on the east flank of Point Arena (fig. 1–1). This San Andreas Fault has an estimated slip rate of about 17 to 25 mm/yr in this area (Bryant and Lundberg, 2002). The last ground rupture in the map area (Brown and Wolfe, 1972) occurred during the devastating great 1906 California earthquake (M7.8, 4/18/1906), thought to have nucleated on the San Andreas Fault about 100 kilometers to the south offshore of San Francisco (for example, Bolt, 1968; Lomax, 2005).

The region between Fort Ross and Point Arena, west of the San Andreas Fault, is the known as the “Gualala Block” on the basis of its distinctive geology (Elder, 1998). The Gualala Block consists of a thick, discontinuous Upper Cretaceous to Miocene stratigraphic section (summarized in Wentworth and others, 1998), however only the Paleocene and Eocene German Rancho Formation (Elder, 1998) is exposed along the coast in the Offshore of Salt Point map area, and this unit is inferred to form all of the rugged seafloor bedrock outcrops in the area. The German Rancho Formation consists of sandstone, mudstone, and conglomerate interpreted as deep-water, submarine-fan deposits (Anderson, 1998). The western boundary of the Gualala Block lies offshore, perhaps at a shore-parallel fault located 3 to 5-km offshore mapped by McCulloch (1987) using seismic-reflection data; this structure was subsequently named the Gualala Fault by Dickinson and others (2005). High-resolution seismic-reflection data (sheet 8, this report) reveal shallow folding and faulting in inferred upper Pleistocene strata along the Gualala Fault trend, suggesting this structure is now or has been recently active.

Publication Summary

This publication about the Offshore of Salt Point map area includes ten map sheets that contain explanatory text, in addition to this descriptive pamphlet and a data catalog of geographic information system (GIS) files. Sheets 1, 2, and 3 combine data from four different sonar surveys to generate comprehensive high-resolution bathymetry and acoustic-backscatter coverage of the map area. These data reveal a range of physiographic features (highlighted in the perspective views on sheet 4) such as the rugged nearshore bedrock outcrop, shallow “scour depressions” filled with coarse-grained sediment, and the flat sediment-covered Salt Point shelf. To validate geological and biological interpretations of the sonar data shown in sheets 1, 2, and 3, the U.S. Geological Survey towed a camera sled over specific offshore locations, collecting both video and photographic imagery; these “ground-truth” surveying data are summarized on sheet 6. Sheet 5 is a “seafloor character” map, which classifies the seafloor on the basis of depth, slope, rugosity (ruggedness), and backscatter intensity, and which is further informed by the ground-truth-survey imagery. Sheet 7 is a map of “potential habitats,” which are delineated on the basis of substrate type, geomorphology, seafloor process, or other attributes that may provide a habitat for a specific species or assemblage of organisms. Sheet 8 compiles representative seismic-reflection profiles from the map area, providing information on the subsurface stratigraphy and structure of the map area. Sheet 9 shows the distribution and thickness of young sediment (deposited over the last about 21,000 years, during the most recent sea-level rise) in both the map area and the larger Salt Point to Drakes Bay region, interpreted on the basis of the seismic-reflection data, and it identifies the Offshore of Salt Point map area as lying within the Salt Point shelf domain. Sheet 10 is a geologic map that

merges onshore geologic mapping (compiled from existing maps by the California Geological Survey) and new offshore geologic mapping that is based on the integration of high-resolution bathymetry and backscatter imagery (sheets 1, 2, 3), seafloor-sediment and rock samples (Reid and others, 2006), digital camera and video imagery (sheet 6), high-resolution seismic-reflection profiles (sheet 8), and air-photo interpretation of the nearshore.

The information provided by the map sheets, pamphlet, and data catalog have a broad range of applications. High-resolution bathymetry, acoustic backscatter, ground-truth-surveying imagery, and habitat mapping all contribute to habitat characterization and ecosystem-based management by providing essential data for delineation of marine protected areas and ecosystem restoration. Many of the maps provide high-resolution baselines that will be critical for monitoring environmental change associated with climate change, coastal development, or other forcings. High-resolution bathymetry is a critical component for modeling coastal flooding caused by storms and tsunamis, as well as inundation associated with longer term, sea-level rise. Seismic-reflection and bathymetric data help characterize earthquake and tsunami sources, critical for natural hazard assessments of coastal zones. Information on sediment distribution and thickness is essential to the understanding of local and regional sediment transport, as well as the development of regional sediment-management plans. In addition, siting of any new offshore infrastructure (for example, pipelines, cables, or renewable-energy facilities) will depend on high-resolution mapping. Finally, this mapping will both stimulate and enable new scientific research and also raise public awareness of, and education about, coastal environments and issues.

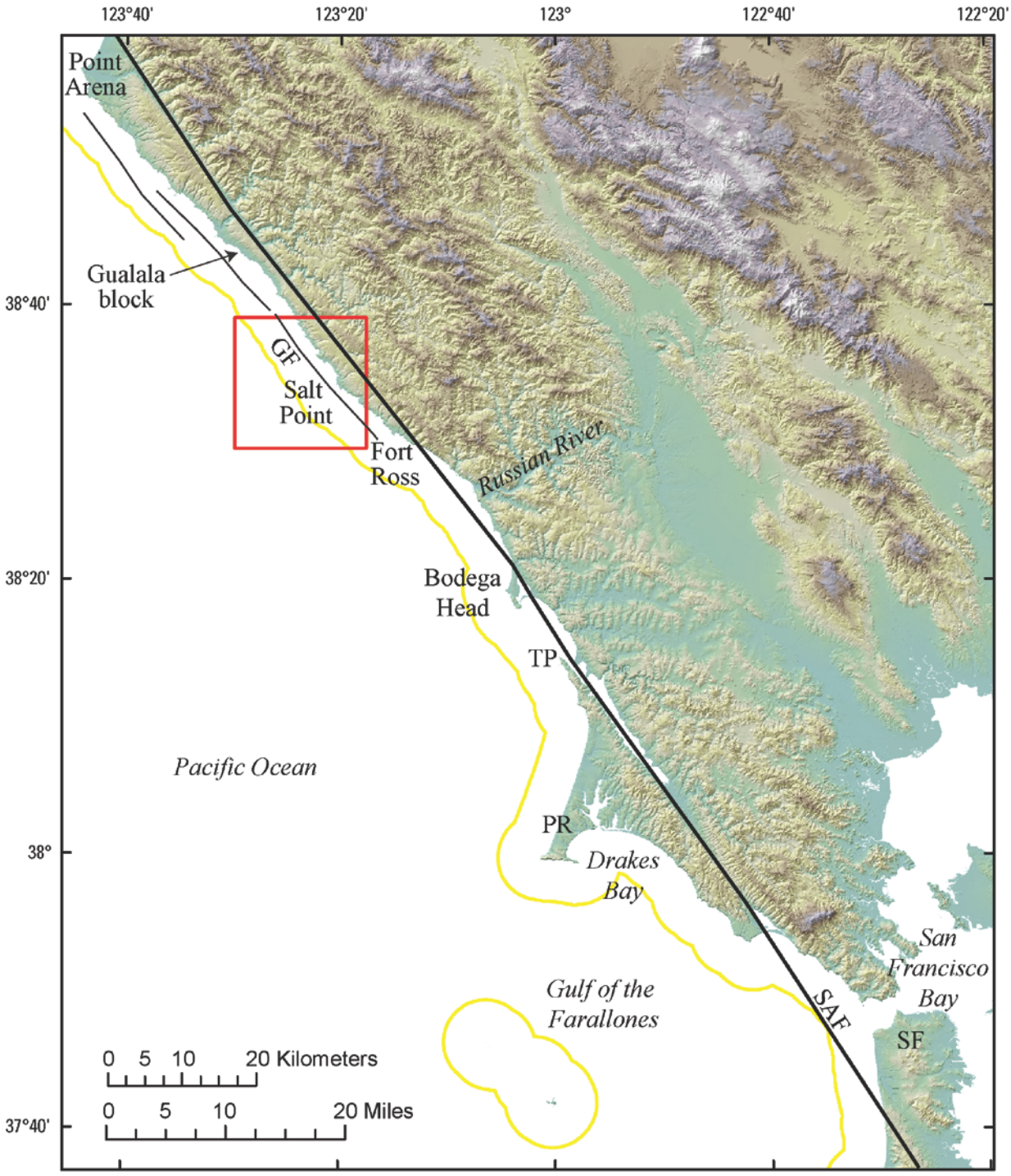

Figure 1–1. Physiography of northern California coast from Point Arena to San Francisco (SF). Red box shows Offshore of Salt Point map area. Abbreviations: GF, Gualala Fault; PR, Point Reyes; SAF, San Andreas Fault; SF, San Francisco; TP, Tomales Point.

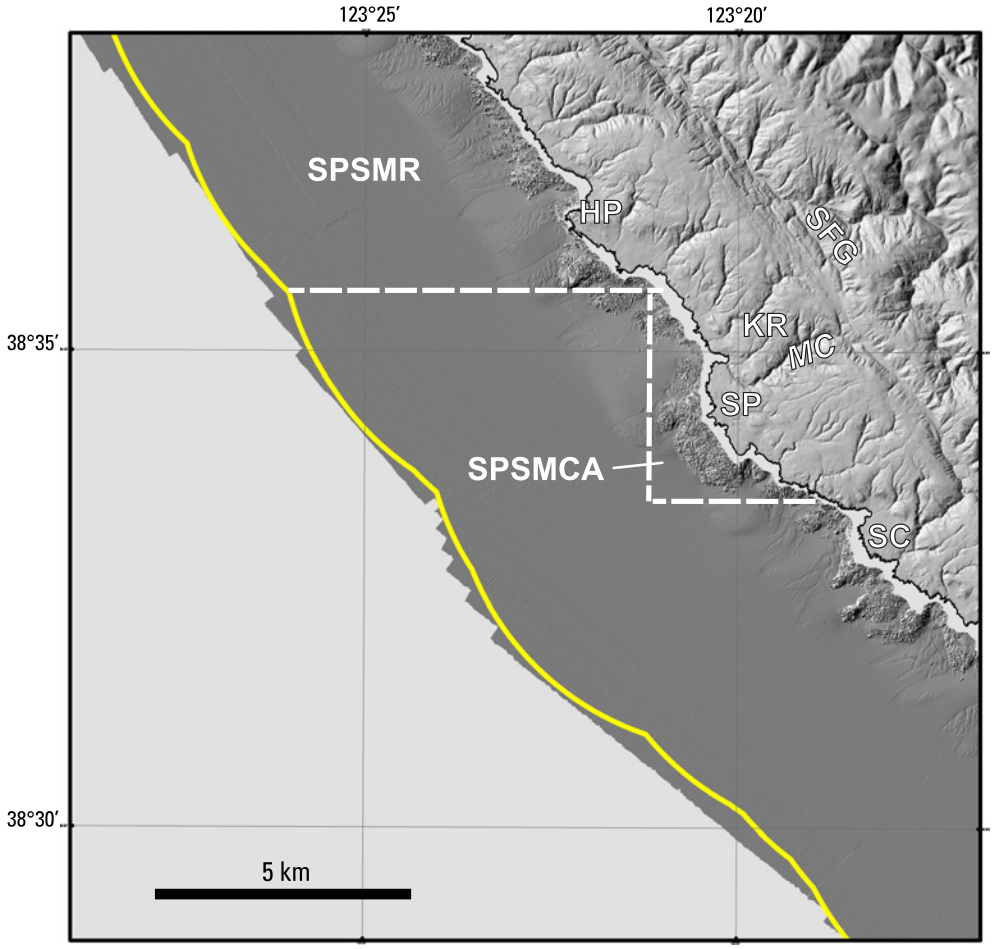

Figure 1–2. Coastal geography of Offshore of Salt Point map area. Yellow line shows limit of California's State Waters. Dashed white lines show southern boundary of Stewarts Point State Marine Reserve (SPSMR) and outer boundaries of Salt Point State Marine Conservation Area (SPSMCA). The Gerstle Cove State Marine Reserve is located within the SPSMCA. Other abbreviations: HP, Horseshoe Point; KR, Kruse Rhododendron State Park; MC, Miller Creek; SFG, South Fork, Gualala River; SC, Stillwater Cove; SP, Salt Point.

Chapter 2. Bathymetry and Backscatter-Intensity Maps of the Offshore of Salt Point Map Area (Sheets 1, 2, and 3)

By Peter Dartnell and Rikk G. Kvitek

The colored shaded-relief bathymetry (sheet 1), the shaded-relief bathymetry (sheet 2), and the acoustic-backscatter (sheet 3) maps of the Offshore of Salt Point map area in northern California were generated from bathymetry and backscatter data collected by California State University, Monterey Bay (CSUMB), and by Fugro Pelagos. Mapping was completed between 2007 and 2010, using a combination of 200-kHz and 400-kHz Reson 7125 and 244-kHz Reson 8101 multibeam echosounders, as well as a 468-kHz SEA SWATHplus bathymetric sidescan-sonar system. These mapping missions combined to collect both bathymetry (sheets 1, 2) and acoustic-backscatter data (sheet 3) from about the 10-m isobath to beyond the 3-nautical-mile limit of California's State Waters.

During the mapping missions, an Applanix POS MV (Position and Orientation System for Marine Vessels) was used to accurately position the vessels during data collection, and it also accounted for vessel motion such as heave, pitch, and roll (position accuracy, ±2 m; pitch, roll, and heading accuracy, ±0.02°; heave accuracy, ±5%, or 5 cm). To account for tidal-cycle fluctuations, CSUMB used NavCom 2050 GPS receiver (CNAV) data, and Fugro Pelagos used KGPS data (GPS data with real-time kinematic corrections); in addition, sound-velocity profiles were collected with an Applied Microsystems (AM) SVPlus sound velocimeter. Soundings were corrected for vessel motion using the Applanix POS MV data, for variations in water-column sound velocity using the AM SVPlus data, and for variations in water height (tides) using vertical-position data from the KGPS receivers.

The multibeam-echosounder backscatter data were postprocessed using CARIS 7.0/Geocoder software. Within Geocoder, the backscatter intensities were radiometrically corrected (including despeckling and angle-varying gain adjustments), and the position of each acoustic sample was geometrically corrected for slant range on a line-by-line basis. After the lines were corrected, they were mosaicked into a 1-m-resolution image. Overlap between parallel lines was resolved using a priority table whose values were based on the distance of each sample from the ship track, with the samples that were closest to and furthest from the ship track being given the lowest priority. An anti-aliasing algorithm was also applied. The mosaics were then exported as georeferenced TIFF images, imported into a geographic information system (GIS), and converted to GRIDs at 2-m resolution.

The SWATHplus backscatter data were postprocessed using USGS software (D.P. Finlayson, written commun., 2011) that normalizes for time-varying signal loss and beam-directivity differences. Thus, the raw 16-bit backscatter data were gain-normalized to enhance the backscatter of the SWATHplus system. The resulting normalized-amplitude values were rescaled to 16-bit and gridded into GeoJPEGs using GRID Processor Software, then imported into a GIS and converted to GRIDs.

Processed soundings from the different mapping missions were exported from the acquisition or processing software as XYZ files and bathymetric surfaces. All the surfaces were merged into one overall 2-m-resolution bathymetric-surface model and clipped to the boundary of the map area. An illumination having an azimuth of 300° and from 45° above the horizon was then applied to the bathymetric surface to create the shaded-relief imagery (sheets 1, 2). In addition, a modified "rainbow" color ramp was applied to the bathymetry data for sheet 1, using reds and oranges to represent shallower depths, and purples to represent greater depths. This colored bathymetry surface was draped over the shaded-relief imagery at 60-percent transparency to create a colored shaded-relief map (sheet 1).

Bathymetric contours (sheets 1, 2, 3, 5, 7, 10) were generated at 10-m intervals from the merged 2-m-resolution bathymetric surface. The merged surface was smoothed using the Focal Mean tool in ArcGIS and a circular neighborhood that has a radius of between 20 and 30 m (depending on the

location). The contours were generated from this smoothed surface using the Spatial Analyst Contour tool in ArcGIS. The most continuous contour segments were preserved; smaller segments and isolated island polygons were excluded from the final output. The contours were then clipped to the boundary of the map area.

The acoustic-backscatter imagery from each different mapping system and processing method were merged into their own individual grids. These individual grids, which cover different areas, were displayed in a GIS to create an acoustic-backscatter map (sheet 3). On the map, brighter tones indicate higher backscatter intensity, and darker tones indicate lower backscatter intensity. The intensity represents a complex interaction between the acoustic pulse and the seafloor, as well as characteristics within the shallow subsurface, providing a general indication of seafloor texture and sediment type. Backscatter intensity depends on the acoustic source level; the frequency used to image the seafloor; the grazing angle; the composition and character of the seafloor, including grain size, water content, bulk density, and seafloor roughness; and some biological cover. Harder and rougher bottom types such as rocky outcrops or coarse sediment typically return stronger intensities (high backscatter, lighter tones), whereas softer bottom types such as fine sediment return weaker intensities (low backscatter, darker tones).

The onshore-area image was generated by applying an illumination having an azimuth of 300° and from 45° above the horizon to 2-m-resolution topographic-lidar data from OpenTopography (available at http://www.opentopography.org/), as well as 10-m-resolution data from the U.S. Geological Survey's National Elevation Dataset (available at http://ned.usgs.gov/).

Chapter 3. Data Integration and Visualization for the Offshore of Salt Point Map Area (Sheet 4)

By Peter Dartnell

Mapping California's State Waters has produced a vast amount of acoustic and visual data, including bathymetry, acoustic backscatter, seismic-reflection profiles, and seafloor video and photography. Researchers use these data to develop maps, reports, and other tools to assist coastal-zone managers and other stakeholders in coastal and marine spatial-planning. For example, seafloor-character (sheet 5), habitat (sheet 7), and geologic (sheet 10) maps of the Offshore of Salt Point map area may assist in the designation of Marine Protected Areas, as well as in their monitoring. These maps and reports also help to analyze environmental change owing to sea-level rise and coastal development, to model and predict sediment and contaminant budgets and transport, to site offshore infrastructure, and to assess tsunami and earthquake hazards. To facilitate this increased understanding and to assist in product development, it is helpful to integrate the different datasets and then view the results in three-dimensional representations such as those displayed on the data integration and visualization sheet for the Offshore of Salt Point map area (sheet 4).

The maps and three-dimensional views on sheet 4 were created using a series of geographic information systems (GIS) and visualization techniques. Using GIS, the bathymetric and topographic data (sheet 1) were converted to ASCIIRASTER format files, and the acoustic-backscatter data (sheet 3) were converted to geoTIFF images. The bathymetric and topographic data were imported in the Fledermaus® software (QPS). The bathymetry was color-coded to closely match the colored shaded-relief bathymetry on sheet 1 in which reds and oranges represent shallower depths and blues represent deeper depths. Topographic data were shown in gray shades. The acoustic-backscatter geoTIFF images were also draped over the bathymetry data. The colored bathymetry, topography, and draped backscatter were then tilted and panned to create the perspective views such as those shown in figures 1, 2, 4, 5, and 6 on sheet 4. These figures highlight the seafloor morphology in the Offshore of Salt Point map area, which includes outcrops of fractured bedrock and complex patterns of shallow depressions.

Video-mosaic images created from digital seafloor video (for example, fig. 3 on sheet 4) display the geologic complexity (rock, sand, and mud; see sheet 10) and biologic complexity (see sheet 11) of the seafloor. Whereas photographs capture high-quality snapshots of smaller areas of the seafloor (see sheet 6), video mosaics capture larger areas and can show transition zones between seafloor environments. Digital seafloor video is collected from a camera sled towed approximately 1 to 2 meters above the seafloor, at speeds of less than 1 nautical mile/hour. Using standard video-editing software, as well as software developed at the Center for Coastal and Ocean Mapping, University of New Hampshire, the digital video is converted to AVI format, cut into 2-minute sections, and desampled to every second or third frame. The frames are merged together using pattern-recognition algorithms from one frame to the next and converted to a TIFF image. The images are then rectified to the bathymetry data using ship navigation recorded with the video and layback estimates of the towed camera sled.

Block diagrams that combine the bathymetry with seismic-reflection-profile data help integrate surface and subsurface observations, especially stratigraphic and structural relations (for example, fig. 6 on sheet 4). These block diagrams were created by converting digital seismic-reflection-profile data (see sheet 8) into TIFF images while taking note of the starting and ending coordinates and maximum and minimum depths. The images were then imported into the Fledermaus® software as vertical images and merged with the bathymetry imagery.

Chapter 4. Seafloor-Character Map of the Offshore of Salt Point Map Area (Sheet 5)

By Mercedes D. Erdey and Guy R. Cochrane

The California State Marine Life Protection Act (MLPA) calls for protecting representative types of habitat in different depth zones and environmental conditions. A science team, assembled under the auspices of the California Department of Fish and Wildlife (CDFW), has identified seven substrate-defined seafloor habitats in California's State Waters that can be classified using sonar data and seafloor video and photography. These habitats include rocky banks, intertidal zones, sandy or soft ocean bottoms, underwater pinnacles, kelp forests, submarine canyons, and seagrass beds. The following five depth zones, which determine changes in species composition, have been identified: Depth Zone 1, intertidal; Depth Zone 2, intertidal to 30 m; Depth Zone 3, 30 to 100 m; Depth Zone 4, 100 to 200 m; and Depth Zone 5, deeper than 200 m (California Department of Fish and Wildlife, 2008). The CDFW habitats, with the exception of depth zones, can be considered a subset of a broader classification scheme of Greene and others (1999) that has been used by the U.S. Geological Survey (USGS) (Cochrane and others, 2003, 2005). These seafloor-character maps are generalized polygon shapefiles that have attributes derived from Greene and others (2007).

A 2007 Coastal Map Development Workshop, hosted by the USGS in Menlo Park, California, identified the need for more detailed (relative to Greene and others' [1999] attributes) raster products that preserve some of the transitional character of the seafloor when substrates are mixed and (or) they change gradationally. The seafloor-character map, which delineates a subset of the CDFW habitats, is a GIS-derived raster product that can be produced in a consistent manner from data of variable quality covering large geographic regions.

The following four substrate classes are identified in the Offshore of Salt Point map area:

- Class I: Fine- to medium-grained smooth sediment
- Class II: Mixed smooth sediment and rock
- Class III: Rock and boulder, rugose
- Class IV: Medium- to coarse-grained sediment (in scour depressions)

The seafloor-character map of the Offshore of Salt Point map area (sheet 5) was produced using video-supervised, maximum-likelihood classification of the bathymetry and intensity of return from sonar systems, following the method described by Cochrane (2008). The two variants used in this classification were backscatter intensity and derivative rugosity. Rugosity calculation was performed using the Terrain Ruggedness (VRM) tool within the Benthic Terrain Modeler toolset v. 3.0 (Wright and others, 2012; available at http://esriurl.com/5754).

Class I, II, and III values were delineated using multivariate analysis. Class IV (medium- to coarse-grained sediment, in scour depressions) values were determined on the basis of their visual characteristics using both shaded-relief bathymetry and backscatter (slight depression in the seafloor, very high backscatter return). The resulting map (gridded at 2 m) was cleaned by hand to remove data-collection artifacts (for example, the trackline nadir).

On the seafloor-character map (sheet 5), the four substrate classes have been colored to indicate the California MLPA depth zones and the Coastal and Marine Ecological Classification Standard (CMECS) slope zones (Madden and others, 2008) in which they belong. The California MLPA depth zones are Depth Zone 1 (intertidal), Depth Zone 2 (intertidal to 30 m), Depth Zone 3 (30 to 100 m), Depth Zone 4 (100 to 200 m), and Depth Zone 5 (greater than 200 m); in the Offshore of Salt Point map area, only Depth Zones 2 and 3 are present. The slope classes that represent the CMECS slope zones are

Slope Class 1 = flat (0° to 5°), Slope Class 2 = sloping (5° to 30°), Slope Class 3 = steeply sloping (30° to 60°), Slope Class 4 = vertical (60° to 90°), and Slope Class 5 = overhang (greater than 90°); in the Offshore of Salt Point map area, only Slope Classes 1 and 2 are present. The final classified seafloor-character raster map image has been draped over the shaded-relief bathymetry for the area (sheets 1 and 2) to produce the image shown on the seafloor-character map on sheet 5.

The seafloor-character classification also is summarized on sheet 5 in table 1. Fine- to medium-grained smooth sediment (sand and mud) makes up 86.9 percent (106.5 km^2) of the map area: 0.3 percent (0.4 km^2) is in Depth Zone 2, and 86.5 percent (106.1 km^2) is in Depth Zone 3. Mixed smooth sediment (sand and gravel) and rock (bedrock with a thin veneer of fine sediment, or rock outcrops having little to no relief) make up 3.6 percent (4.4 km^2) of the map area: 0.9 percent (1.1 km^2) is in Depth Zone 2, and 2.7 percent (3.3 km^2) is in Depth Zone 3. Rock and boulder, rugose (rock outcrops and boulder fields having high surficial complexity) makes up 5.8 percent (7.2 km^2) of the map area: 3.1 percent (3.9 km^2) is in Depth Zone 2, and 2.7 percent (3.3 km^2) is in Depth Zone 3. Medium- to coarse-grained sediment (in scour depressions consisting of material that is coarser than the surrounding seafloor) makes up 3.7 percent (4.5 km^2) of the map area: less than 0.1 percent (<0.1 km^2) is in Depth Zone 2 and 3.7 percent (4.5 km^2) is in Depth Zone 3.

A small number of video observations were used to supervise the numerical classification of the seafloor. All video observations (see sheet 6) are used for accuracy assessment of the seafloor-character map after classification To compare observations to classified pixels, each observation point is assigned a class (I, II, or III), according to the visually derived, major or minor geologic component (for example, sand or rock) and the abiotic complexity (vertical variability) of the substrate recorded during ground-truth surveys (table 4–1; see also, chapter 5 of this pamphlet). Class IV values were assigned on the basis of the observation of one or more of a group of features that includes both larger scale bedforms (for example, sand waves), as well as sediment-filled scour depressions that resemble the “rippled scour depressions” of Cacchione and others (1984) and Phillips and others (2007) and also the “sorted bedforms” of Murray and Thieler (2004), Goff and others (2005), and Trembanis and Hume (2011). On the geologic map (see sheet 10 of this report), they are referred to as “marine shelf scour depressions.”

Next, circular buffer areas were created around individual observation points using a 10-m radius to account for layback and positional inaccuracies inherent to the towed-camera system. The radius length is an average of the distances between the positions of sharp interfaces seen on both the video (the position of the ship at the time of observation) and sonar data, plus the distance covered during a 10-second observation period at an average speed of 1 nautical mile/hour. Each buffer, which covers more than 300 m^2, contains approximately 77 pixels. The classified (I, II, III) buffer is used as a mask to extract pixels from the seafloor-character map. These pixels are then compared to the class of the buffer. For example, if the shipboard-video observation is Class II (mixed smooth sediment and rock), but 12 of the 77 pixels within the buffer area are characterized as Class I (fine- to medium-grained smooth sediment), and 15 (of the 77) are characterized as Class III (rock and boulder, rugose), then the comparison would be “Class I, 12; Class II, 50; Class III, 15” (fig. 4–1). If the video observation of substrate is Class II, then the classification is accurate because the majority of seafloor pixels in the buffer are Class II. The accuracy values in table 4–2 represent the final of several classification iterations aimed at achieving the best accuracy, given the variable quality of sonar data (see discussion in Cochrane, 2008) and the limited ground-truth information available when compared to the continuous coverage provided by swath sonar. Presence/absence values in table 4–2 reflect the percentages of observations where the sediment classification of at least one pixel within the buffer zone agreed with the observed sediment type at a certain location.

The seafloor in the Offshore of Salt Point map area is covered predominantly by Class I sediment composed of sand and mud. Several exposures of rugose bedrock (Class III) are present in the nearshore (< 60 m water depth) area. The rock outcrops are covered with varying thicknesses of fine (Class I) to

coarse (Class II) sediment. Several areas of medium- to coarse-grained scour depressions (Class IV) also have been identified adjacent to rock outcrops.

The classification accuracy of Class I, Class III, and Class IV (86 percent, 92 percent, and 59 percent accurate, respectively; table 4–2) is determined by comparing the shipboard video observations and the classified map. A single video observation was available for Class II (mixed smooth sediment and rock) and this one observation contained 18 percent of Class II pixels within the 10-meter buffer zone. Bedrock outcrops in this area are composed of differentially eroded sedimentary rocks. Erosion of softer layers produces Class I and II sediments, resulting in patchy areas of rugose rock and boulder habitat (Class III) on the seafloor. A single buffered observation locale of 78 pixels, therefore, is likely to be interspersed with other classes of pixels, in addition to Class III. Percentages for presence/absence within a buffer also were calculated as a better measure of the accuracy of classification for patchy habitats. The presence/absence accuracy was found to be significant for all classes (88 percent for Class I, 100 percent for Class II, 100 percent for Class III, and 66 percent for Class IV).

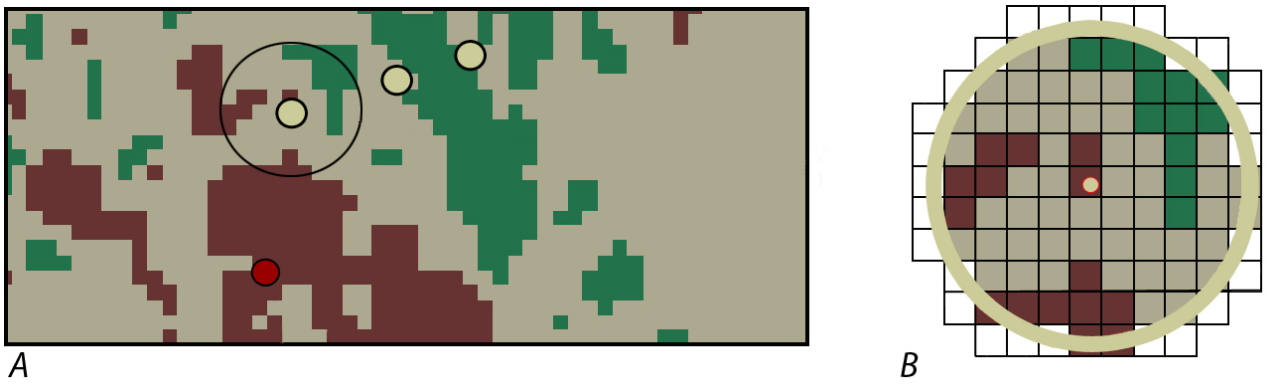

Figure 4–1. Detailed view of ground-truth data, showing accuracy-assessment methodology. *A*, Dots illustrate ground-truth observation points, each of which represents 10-second window of substrate observation plotted over seafloor-character grid; circle around dot illustrates area of buffer depicted in *B*. *B*, Pixels of seafloor-character data within 10-m-radius buffer centered on one individual ground-truth video observation.

Table 4–1. Conversion table showing how video observations of primary substrate (more than 50 percent seafloor coverage), secondary substrate (more than 20 percent seafloor coverage), and abiotic seafloor complexity (in first three columns) are grouped into seafloor-character-map Classes I, II, III, and IV for use in supervised classification and accuracy assessment in the Offshore of Salt Point map area.

[In areas of low visibility where primary and secondary substrate could not be identified with confidence, recorded observations of substrate (in fourth column) were used to assess accuracy]

Primary-substrate component	Secondary-substrate component	Abiotic seafloor complexity	Low-visibility observations
Class I			
mud	mud	low	
mud	sand	low	
sand	mud	low	
sand	sand	low	
			sediment
			mud component
			ripples
Class II			
sand	rock	moderate	
Class III			
boulders	rock	high	
rock	rock	moderate	
rock	rock	high	
rock	sand	moderate	
Class IV			
gravel	sand	low	
sand	sand	low	
			megaripples
			oscillatory megaripples
			depression

Table 4–2. Accuracy-assessment statistics for seafloor-character-map classifications in Offshore of Salt Point map area.

[Accuracy assessments are based on video observations]

Class	Number of observations	% majority	% presence/absence
I—Fine- to medium-grained smooth sediment	170	85.5	88.2
II—Mixed smooth sediment and rock	1	17.5	100.0
III—Rock and boulder, rugose	18	92.4	100.0
IV—Medium- to coarse-grained sediment (in scour depressions)	32	58.9	65.6

Chapter 5. Ground-Truth Studies for the Offshore of Salt Point Map Area (Sheet 6)

By Nadine E. Golden and Guy R. Cochrane

To validate the interpretations of sonar data in order to turn it into geologically and biologically useful information, the U.S. Geological Survey (USGS) towed a camera sled (fig. 5–1) over specific locations throughout the Offshore of Salt Point map area to collect video and photographic data that would "ground truth" the seafloor. This ground-truth surveying occurred in 2008. The camera sled was towed 1 to 2 m above the seafloor at speeds of between 1 and 2 nautical miles/hour. Ground-truth surveys in this map area include approximately 5 trackline kilometers of video and 674 still photographs, in addition to 244 recorded seafloor observations of abiotic and biotic attributes. A visual estimate of slope also was recorded.

Figure 5–1. Photograph of camera sled used in USGS 2008 ground-truth survey.

During the cruise, the USGS camera sled housed two standard-definition (640×480 pixel resolution) video cameras (one forward looking and one downward looking), a high-definition (1,080×1,920 pixel resolution) video camera, and an 8-megapixel digital still camera. During this cruise, in addition to recording the seafloor characteristics, a digital still photograph was captured once every 30 seconds.

The camera-sled tracklines (shown by colored dots on the map on sheet 6) are sited in order to visually inspect areas representative of the full range of bottom hardness and rugosity in the map area. The video is fed in real time to the research vessel, where USGS and National Oceanic and Atmospheric Administration (NOAA) scientists record both the geologic and biologic character of the seafloor. While the camera is deployed, several different observations are recorded for a 10-second period once every minute, using the protocol of Anderson and others (2007). Observations of primary substrate, secondary substrate, slope, abiotic complexity, biotic complexity, and biotic cover are mandatory. Observations of key geologic features and the presence of key species also are made.

Primary and secondary substrate, by definition, constitute greater than 50 and 20 percent of the seafloor, respectively, during an observation. The grain-size values that differentiate the substrate classes are based on the Wentworth (1922) scale, and the sand, cobble, and boulder sizes are classified

as in Wentworth (1922). However, the difficulty in distinguishing the finest divisions in the Wentworth (1922) scale during video observations made it necessary to aggregate some grain-size classes, as was done in the Anderson and others (2007) methodology: the granule and pebble sizes have been grouped together into a class called “gravel,” and the clay and silt sizes have been grouped together into a class called “mud.” In addition, hard bottom and clasts larger than boulder size are classified as “rock.” Benthic-habitat complexity, which is divided into abiotic (geologic) and biotic (biologic) components, refers to the visual classification of local geologic features and biota that potentially can provide refuge for both juvenile and adult forms of various species (Tissot and others, 2006).

Sheet 6 contains a smaller, simplified (depth-zone symbology has been removed) version of the seafloor-character map on sheet 5. On this simplified map, the camera-sled tracklines used to ground-truth-survey the sonar data are shown by aligned colored dots, each dot representing the location of a recorded observation. A combination of abiotic attributes (primary- and secondary-substrate compositions), as well as vertical variability were used to derive the different classes represented on the seafloor-character map (sheet 5); on the simplified map, the derived classes are represented by colored dots. Also on this map are locations of the detailed views of seafloor character, shown by boxes (Boxes A through F); for each view, the box shows the locations (indicated by colored stars) of representative seafloor photographs. For each photograph, an explanation of the observed seafloor characteristics recorded by USGS and NOAA scientists is given. Note that individual photographs often show more substrate types than are reported as the primary and secondary substrate. Organisms, when present, are labeled on the photographs.

The ground-truth survey is designed to investigate areas that represent the full spectrum of high-resolution multibeam bathymetry and backscatter-intensity variation. Figure 5–2 shows that, in the Offshore of Salt Point map area, the seafloor surface is predominately comprised of sand and mud. The seafloor character map (sheet 5) shows that the Offshore of Salt Point map area is also characterized by extensive onshore-offshore rock outcrops associated with uplift along faults that cross the shoreline from the seafloor in the south to on land in this map area (sheet 10). Rocks exposed in this area are massive and predominantly consist of sandstone. Rocky habitat spans the entire wave-exposed coast and extends about one nautical mile offshore. Areas of coarse sediments in ripple scour depressions, generated by localized-strong bottom currents, extend offshore from the rocky areas. The remaining deeper area of California’s State Waters is sand and muddy sand habitat.

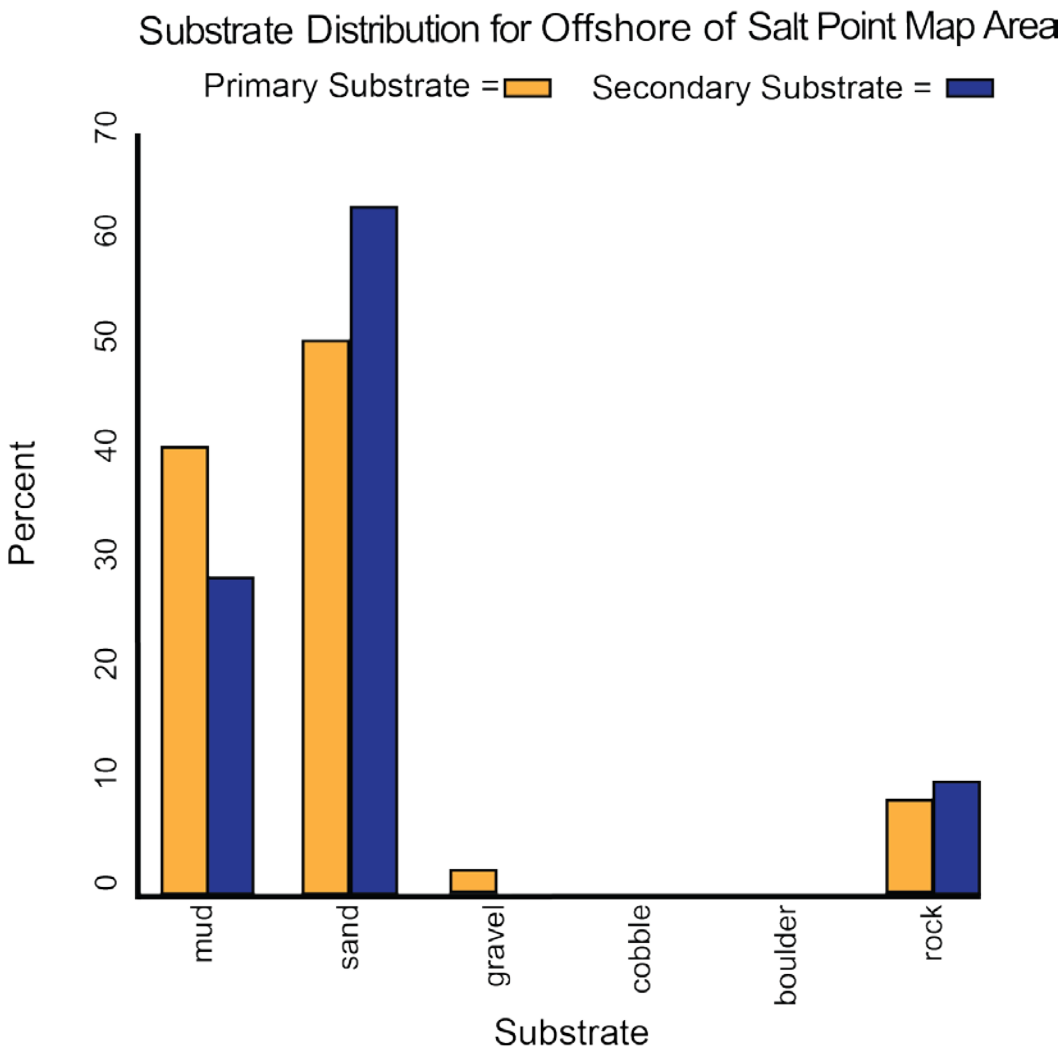

Figure 5–2. Graph showing distribution of primary and secondary substrate determined from video observations in Offshore of Salt Point map area.

Chapter 6. Potential Marine Benthic Habitats of the Offshore of Salt Point Map Area (Sheet 7)

By H. Gary Greene, Charles A. Endris, and Bryan E. Dieter

The map on sheet 7 shows "potential" marine benthic habitats in the Offshore of Salt Point map area, representing a substrate type, geomorphology, seafloor process, or any other attribute that may provide a habitat for a specific species or assemblage of organisms. This map, which is based largely on seafloor geology, also integrates information displayed on several other thematic maps of the Offshore of Salt Point map area. High-resolution sonar bathymetry data, converted to depth grids (seafloor DEMs; sheet 1), are essential to development of the potential marine benthic habitat map, as is shaded-relief imagery (sheet 2), which allows visualization of seafloor terrain and provides a foundation for interpretation of submarine landforms.

Backscatter maps (sheet 3) also are essential for developing potential benthic habitat maps. High backscatter is further indication of "hard" bottom, consistent with interpretation as rock or coarse sediment. Low backscatter, indicative of a "soft" bottom, generally indicates a fine-sediment environment. Habitat interpretations also are informed by actual seafloor observations from ground-truth surveying (sheet 6), by seafloor-character maps that are based on video-supervised maximum-likelihood classification (sheet 5), and by seafloor-geology maps (sheet 10). The habitat interpretations on sheet 7 are further informed by the usSEABED bottom-sampling compilation of Reid and others (2006).

Broad, generally smooth areas of seafloor that lack sharp and angular edge characteristics are mapped as "sediment;" these areas may be further defined by various sedimentary features (for example, erosional scours and depressions) and (or) depositional features (for example, dunes, mounds, or sand waves). In contrast, many areas of seafloor bedrock exposures are identified by their common sharp edges and high relative relief; these may be contiguous outcrops, isolated parts of outcrop protruding through sediment cover (pinnacles or knobs), or isolated boulders. In many locations, areas within or around a rocky feature appear to be covered by a thin veneer of sediment; these areas are identified on the habitat map as "mixed" induration (that is, containing both rock and sediment). The combination of remotely observed data (for example, high-resolution bathymetry and backscatter, seismic-reflection profiles) and directly observed data (for example, camera transects, sediment samples) translates to higher confidence in the ability to interpret broad areas of the seafloor.

To avoid any possible misunderstanding of the term "habitat," the term "potential habitat" (as defined by Greene and others, 2005) is used herein to describe a set of distinct seafloor conditions that in the future may qualify as an "actual habitat." Once habitat associations of a species are determined, they can be used to create maps that depict actual habitats, which then need to be confirmed by "ground-truth" surveying using in situ observations, video, and (or) photographic documentation.

Classifying Potential Marine Benthic Habitats

Potential marine benthic habitats in the Offshore of Salt Point map area are mapped using the Benthic Marine Potential Habitat Classification Scheme, a mapping-attribute code developed by Greene and others (1999, 2007). This code, which has been used previously in other offshore California areas (see, for example, Greene and others, 2005, 2007), was developed to easily create categories of marine benthic habitats that can then be queried within a GIS or a database. The code contains several categories that can be subdivided relative to the spatial scale of the data. The following categories can be applied directly to habitat interpretations determined from remote-sensing imagery collected at a scale of tens of kilometers to one meter: Megahabitat, Seafloor Induration, Meso/Macrohabitat, Modifier, Seafloor Slope, Seafloor Complexity, and Geologic Unit. Additional categories of Macro/Microhabitat,

Seafloor Slope, and Seafloor Complexity, and Geologic Attribute can be applied to habitat interpretations determined from seafloor samples, video, still photographs, or direct observations at a scale of 10 meters to a few centimeters. These two scale-dependent groups of categories can be used together, to define a habitat across spatial scales, or separately, to compare large- and small-scale habitat types.

The four categories and their attribute codes that are used on the Offshore of Salt Point map area are explained in detail below (note, however, that not all categories may be used in a particular map area, given the study objectives, data availability, or data quality); attribute codes in each category are depicted on the map by the letters and, in some cases, numbers that make up the map-unit symbols:

Megahabitat—Based on depth and general physiographic boundaries; used to distinguish features on a scale of tens of kilometers to kilometers. Depicted on map by capital letter, listed first in map-unit symbol; generalized depth ranges are given below:

E = Estuary (0 to 100 m)

S = Shelf; continental and island shelves (0 to 200 m)

Seafloor Induration—Refers to substrate hardness. Depicted on map by lower-case letter, listed second in map-unit symbol; may be further subdivided into distinct sediment types, depicted by lower-case letter(s) in parentheses, listed immediately after substrate hardness; multiple attributes listed in general order of relative abundance, separated by slash; queried where inferred.

h = Hard bottom (for example, rock outcrop or sediment pavement)

m = Mixed hard and soft bottom (for example, local sediment cover of bedrock)

s = Soft bottom; sediment cover

(b) = Boulders

(g) = Gravel

(s) = Sand

(m) = Mud, silt, and (or) clay

Meso/Macrohabitat—Related to scale of habitat; consists of seafloor features one kilometer to one meter in size. Depicted on map by lower-case letter and, in some cases, additional lower-case letter in parentheses, listed third in map-unit symbol; multiple attributes separated by slash.

b = Beach, relic (submerged) or shoreline

(b)/p = Pinnacle indistinguishable from boulder

d = Deformed, tilted and (or) folded bedrock; overhang

e = Exposure; bedrock

h = Hole; depression

m = Mound; linear ridge

p = Pinnacle; cone

s = Scarp, cliff, fault, or slump scar

w = Dynamic bedform

y = Delta; fan

Modifier—Describes texture, bedforms, biology, or lithology of seafloor. Depicted on map by lower-case letter, in some cases followed by additional lower-case letter(s) either after hyphen or in parentheses (or both), following an underscore; multiple attributes separated by slash.

_a = Anthropogenic (artificial reef, breakwall, shipwreck, disturbance)

_a-dg = Dredge groove or channel

_a-g = Groin, jetty, rip-rap

_a-w = Wreck, ship, barge, or plane

_c = Consolidated sediment (claystone, mudstone, siltstone, sandstone, breccia, or conglomerate)

_d = Differentially eroded
_f = Fracture, joint; faulted
_g = Granite
_h = Hummocky, irregular relief
_r = Ripple (amplitude, greater than 10 cm)
_s = Scour (current or ice; direction noted)
_u = Unconsolidated sediment

Examples of Attribute Coding

To illustrate how these attribute codes can be used to describe remotely sensed data, the following examples are given:

Ss(s)_u = Soft unconsolidated sediment (sand) on continental shelf.
Es(s/m)_r/u = Rippled, soft, unconsolidated sediment (sand and mud) in estuary.
She_g = Hard rock outcrop (granite) on continental shelf.

Map Area Habitats

Delineated in the Offshore of Salt Point map area are 7 potential marine benthic habitat types, covering 122.69 km^2. These habitat types range from unconsolidated continental shelf sediments (4 habitat types), to mixed substrate on the continental shelf (1 habitat type), to hard substrate on continental shelf (2 habitat types). In the total area mapped the dominant habitat type was unconsolidated sediment that covered 113.14 km^2 (92.2 percent) with hard rock covering 9.33 km^2 (7.6 percent), and sediment covered bedrock covering 0.23 km^2 (0.2 percent). Rock outcrops and rubble are considered the primary habitat types for rockfish and lingcod (Cass and others, 1990; Love and others, 2002), both of which are recreationally and commercially important species.

Chapter 7. Subsurface Geology and Structure of the Offshore of Salt Point Map Area and the Salt Point to Drakes Bay Region (Sheets 8 and 9)

By Samuel Y. Johnson, Stephen R. Hartwell, Janet T. Watt, and Ray W. Sliter

The seismic-reflection profiles presented on sheet 8 provide a third dimension, depth, to complement the surficial seafloor-mapping data already presented (sheets 1 through 7) for the Offshore of Salt Point map area. These data, which are collected at several resolutions, extend to varying depths in the subsurface, depending on the purpose and mode of data acquisition. The seismic-reflection profiles (sheet 8) provide information on sediment character, distribution, and thickness, as well as potential geologic hazards, including active faults, areas prone to strong ground motion, and tsunamigenic slope failures. The information on faults provides essential input to national and state earthquake-hazard maps and assessments (for example, Petersen and others, 2008).

The maps on sheet 9 show the following interpretations, which are based on the seismic-reflection profiles on sheet 8: the thickness of the two uppermost sediment units; the depth to base of these two units; and both the local and regional distribution of faults and earthquake epicenters (data from U.S. Geological Survey, 2010; Northern California Earthquake Data Center, 2014).

Data Acquisition

Most profiles displayed on sheet 8 (figs. 1, 2, 3, 4, 6, 7, 9, 10) were collected in 2009 on U.S. Geological Survey (USGS) cruise S–8–09–NC. The single-channel seismic-reflection data were acquired using the SIG 2Mille minisparker that used a 500-J high-voltage electrical discharge fired 1 to 4 times per second, which, at normal survey speed of 4 to 4.5 nautical miles/hour, gives a data trace every 0.5 to 2.0 m of lateral distance covered. The data were digitally recorded in standard SEG-Y 32-bit floating-point format using Triton Subbottom Logger (SBL) software that merges seismic-reflection data with differential GPS-navigation data. After the survey, a short-window (20 ms) automatic gain control algorithm was applied to the data, along with a 160- to 1,200-Hz bandpass filter and a heave correction that uses an automatic seafloor-detection window (averaged across 30 m of lateral distance covered). These high-resolution data can resolve geologic features that are a few meters thick (small-scale features) to subbottom depths of about 400 m.

Figures 5 and 8 on sheet 8 show deep-penetration, depth-migrated, multichannel seismic-reflection profiles collected in 1982 by WesternGeco on cruise W–4–82–NC. These profiles and other similar data were collected in many areas offshore of California in the 1970s and 1980s when these areas were considered a frontier for oil and gas exploration. Most of these data have been publicly released and are now archived at the U.S. Geological Survey National Archive of Marine Seismic Surveys (U.S. Geological Survey, 2009). These data were acquired using a large-volume air-gun source that has a frequency range of 3 to 40 Hz and recorded with a multichannel hydrophone streamer about 2 km long. Shot spacing was about 30 m. These data can resolve geologic features that are 20 to 30 m thick, down to subbottom depths of about 4 km.

Seismic-Reflection Imaging of the Continental Shelf

Sheet 8 shows seismic-reflection profiles in the Offshore of Salt Point map area. The seafloor in this area extends from the shoreline to water depths of about 90 to 100 m. The nearshore to inner shelf area (to water depths of about 50 to 60 m) typically dips seaward about 1.0° to 1.5° and is underlain by rocky outcrops of the Tertiary German Rancho Formation and sand-sized to coarser grained sediment

(sheet 10). The midshelf, underlain predominantly by muddy sediments, slopes more gently, generally less than 0.5°. Surficial and shallow sediments were deposited during the sea-level fall (about 30,000 to 21,000 years ago) associated with the Last Glacial Maximum (LGM), and the subsequent ongoing post–LGM sea-level rise (Fairbanks, 1989; Fleming and others, 1998; Lambeck and Chappell, 2001; Peltier and Fairbanks, 2006). Sea level was about 125 m lower than present during the LGM, at which time the Offshore of Salt Point map area was emergent and the shoreline was about 20 km west of its present location. Post–LGM sea-level rise was rapid, about 9 to 11 meters per thousand years, until about 7,000 years ago when it slowed considerably to about 1 meter per thousand years (Peltier and Fairbanks, 2006; Stanford and others, 2011). Sea-level rise lead to broadening of the continental shelf, progressive eastward migration of the shoreline and wave-cut platform, and associated transgressive erosion and deposition (see, for example, Catuneanu, 2006).

Sediments inferred to have been deposited during pre–LGM sea-level fall and the post–LGM sea-level rise (the rapid transgression and post-about 7 ka highstand) are shaded pink and blue, respectively, in the high-resolution seismic-reflection profiles on sheet 8 (figs. 1, 2, 3, 4, 6, 7, 9, 10) and composite sediment thickness is shown on Sheet 9. These sediments, supplied primarily from the mouth of the Russian River (about 15 km south of the map area) and local coastal watersheds, were deposited above a sharp transgressive surface of erosion (see, for example, Catuneanu, 2006) commonly marked by minor channeling, and an upward change to lower amplitude, more diffuse reflections. These relatively lower-amplitude reflections typically have low to high frequency, parallel to divergent geometries, and are continuous to moderately continuous (terminology from Mitchum and others, 1977). The relatively low amplitude may partly result from extensive winnowing from full Pacific Ocean wave energy and currents, resulting in uniform sediment grain size. These conditions tend to minimize the acoustic impedance contrasts needed to produce seismic reflections with higher amplitudes.

Strata beneath the two uppermost Pleistocene and Holocene units and above the German Rancho Formation are represented on sheet 8 (figs. 1, 2, 3, 4, 6, 7, 9, 10) by low-to-high amplitude, high-frequency, parallel to subparallel, continuous reflections. Reflections are commonly flat to gently folded and dip less than 10° (though they appear much steeper because of the 12.5:1 vertical exaggeration). The upper contact with the two uppermost stratigraphic units ranges from angular (where the lower unit has been folded) to parallel or subparallel. These strata are inferred to be Pleistocene in age (marine isotope stage 3 and older; Waelbroeck and others, 2002) because (1) they underlie inferred uppermost Pleistocene and Holocene (marine isotope stages 1 and 2) strata, and (2) because their horizon can be traced continuously with other data from USGS cruise S–8–09–NC to the Quaternary section penetrated in Shell borehole P-027-1 (Heck and others, 1990), located 15 km south of the map area. Similar to the overlying Pleistocene and Holocene deposits, these strata represent wave-reworked deltaic and shelf sediments derived primarily from the Russian River. Reflections from this interval are locally obscured by interstitial gas within the sediment (see, for example, figs. 7, 9, 10 on sheet 8), an effect that has been referred to as “gas blanking,” “acoustic turbidity,” or “acoustic masking” (Hovland and Judd, 1988; Fader, 1997). Interstitial gas scatters or attenuates acoustic energy, preventing penetration. Local “bright spot” reflections with notably high amplitudes highlight gas-charged sediments on a few seismic-reflection lines, most notably imaged at the crest of a shallow anticline shown on profile PR-122 (see fig. 10 on sheet 8).

Bedrock of the German Rancho Formation crops out onland and in the nearshore along the coast of the Offshore of Salt Point map area (sheet 10). The nearshore bedrock is cut by numerous faults and has moderate to steep dips. The unit appears massive and “reflection-free” on high-resolution seismic-reflection data (for example, figs. 2, 3. 4, 6, 7, 9 on sheet 8) and forms an “acoustic basement” for overlying Quaternary sediments. On higher-energy, industry seismic profiles (see figs. 5, 8 on sheet 8), basement rocks of probable Tertiary age are characterized by low- to high-amplitude, parallel to divergent, continuous reflections.

Geologic Structure and Recent Deformation

Local faulting, folding, uplift, and subsidence have also influenced coastal and shelf morphology and evolution in the Offshore of Salt Point map area. The shoreline in the map area is located about two kilometers west of the San Andreas Fault Zone, the transform boundary between the Pacific and North American tectonic plates. The San Andreas Fault extends offshore about 5 km south of the map area near Fort Ross, and about 50 km north of the map area on the east flank of Point Arena. The coast between Fort Ross and Point Arena, west of the San Andreas Fault, is the known as the "Gualala Block" (fig. 8–1; Elder, 1998) on the basis of its distinctive geology, which has been used to develop Neogene paleogeographic reconstructions of coastal California that restore as much as 150 to 180 km of right-lateral slip (see, for example, Wentworth, 1968; Wentworth and others, 1998; Jachens and others, 1998; Dickinson and others, 2005; Burnham, 2009) on the combined San Andreas and San Gregorio Fault systems. The Gualala Block is underlain by a thick (as much as 9 to 11 km, in aggregate), discontinuous Upper Cretaceous to Miocene stratigraphic section (summarized in Wentworth and others, 1998), however only the Paleocene and Eocene German Rancho Formation is exposed onshore in this map area and, as described in the previous section, represents local "acoustic basement."

The western boundary of the Gualala Block is located offshore. Using seismic-reflection data, McCulloch (1987; his fig. 14) mapped a shore-parallel fault about 3 to 5 km offshore. Jachens and others (1998) evaluated aeromagnetic and gravity data across this zone and modeled this structure as a steep fault within the Salinian basement block, characterized by 3 to 5 km of right-lateral offset. Subsequently, Dickinson and others (2005) named this structure the Gualala Fault and suggested it was a late Miocene strand of the San Andreas Fault separating Franciscan Complex and Salinian basement blocks, with minimum right-lateral slip of 70 km. Deep industry seismic-reflection data within California's State Waters show the Gualala Fault as a steep, northeast-dipping fault (figs. 5, 8 on sheet 8) and do not distinguish between these hypotheses.

Shallower, high-resolution seismic-reflection profiles, crossing the Gualala Fault from southwest to northeast, show two deformation zones of faulted and folded upper Pleistocene strata above the Gualala Fault: the "Gualala Fault deformation zone" and a more nearshore "east Gualala deformation zone" (see sheet 10). Faults in these zones are identified and mapped based on abrupt truncation or warping of reflections and (or) juxtaposition of reflection panels with different seismic parameters such as reflection presence, amplitude, frequency, geometry, continuity, and vertical sequence. Faults cut and (or) are aligned with many fold axes, and faulting is a clear control on fold development. Both faults and folds trend northwest, parallel to the shoreline and fold limbs typically dip 5° or less. There is notable stratigraphic thinning between synclinal troughs and anticlinal crests indicating that deposition occurred as the folds grew ("growth folding"). For example, figure 1 of sheet 8 shows 32 m of stratigraphic thinning over a horizontal distance of 1,400 m (between reflections "1" and "2"). The pervasive deformation of Pleistocene strata and the overall pattern of faulting and folding (sheet 10) suggests recently active (last 100,000 years?) northwest shortening above a northeast-dipping fault zone that may include one or more blind fault splays.

Map E on sheet 9 shows the regional pattern of major faults and earthquakes. Fault location is simplified and compiled from our mapping within California's State Waters (see sheet 10) and from the U.S. Geological Survey's Quaternary fault and fold database (U.S. Geological Survey and California Geological Survey, 2010). Earthquake epicenters are from the Northern California Earthquake Data Center (2014), which is maintained by the U.S. Geological Survey and the University of California, Berkeley, Seismological Laboratory; all events of magnitude 2.0 and greater for the time period 1967 through March 2014 are shown. The largest earthquake in the map area (M3.7, 7/6/2006) was located about 13 km offshore. A notable lack of microseismicity on the adjacent San Andreas Fault has occurred since the devastating great 1906 California earthquake (M7.8, 4/18/1906), thought to have nucleated on

the San Andreas Fault offshore of San Francisco (see, for example, Bolt, 1968; Lomax, 2005), about 100 km south of the map area.

Thickness and Depth to Base of Uppermost Pleistocene and Holocene Deposits

Maps on sheet 9 show the thickness and the depth to base of uppermost Pleistocene and Holocene (post-LGM) deposits (blue- and pink-shaded units of seismic-reflection profiles; sheet 8) both for the Offshore of Salt Point map area (Maps A, B) and, to establish regional context, for a larger area (about 115 km of coast) that extends from the Salt Point area south to the southern part of the Point Reyes peninsula (Maps C, D). To make these maps, water bottom and depth to base of the LGM horizons were mapped from seismic-reflection profiles using Seisworks software. The difference between the two horizons was exported from Seisworks for every shot point as XY coordinates (UTM zone 10) and two-way travel time (TWT). The thickness of the composite sedimentary unit (Maps C, D) was determined by applying a sound velocity of 1,600 m/sec to the TWT. The thickness points were interpolated to a preliminary continuous surface, overlaid with zero-thickness bedrock outcrops (see sheet 10), and contoured following the methodology of Wong and others (2012).

Several factors required manual editing of the preliminary sediment-thickness maps to make the final product. The Gualala, Point Reyes, and San Andreas Faults disrupt the sediment sequence in the region (Maps D, E on sheet 9). The thickness data points are dense along tracklines (about 1 m apart) and sparse between tracklines (1 km apart), resulting in minor contouring artifacts. To incorporate the effect of the faults, to remove irregularities from interpolation, and to reflect other geologic information and complexity, the resulting interpolated contours were modified. Contour modifications and regridding were repeated several times to produce the final regional sediment-thickness map (Wong and others, 2012). Information for the depth to base of the composite uppermost Pleistocene and Holocene sediment unit (Maps A, C on sheet 9) was generated by adding the thickness data to water depths determined by multibeam bathymetry (see sheet 1).

The thickness of the composite uppermost Pleistocene and Holocene sedimentary unit in the Offshore of Salt Point map area ranges from 0 to 23 m (Map B on sheet 9), and the depth to the base of this composite unit ranges from 0 to about 107 m (Map A on sheet 9). Mean sediment thickness for the map area is 12.1 m, and the total sediment volume is $1{,}226 \times 10^6\ m^3$ (table 7–1). Most of the seafloor within about 1 km of the shoreline (to water depths of about 30 to 50 m) consists of bedrock outcrops with little or no sediment cover except in a few areas at the mouths of coastal watersheds such as Miller Creek on the north flank of Salt Point (fig. 1–2), where fluvial channels eroded through bedrock during late Quaternary sea-level lowstand(s).

There are two notable zones of increased sediment thickness in the map area (Map B on sheet 9). The first zone is about 1 km wide and parallels the shore north of Salt Point at water depths of about 50 m. The thickness of this zone largely results from the presence of a downlapping sediment wedge (pink shaded unit on fig. 1) that accumulated along the southwest flank of the nearshore bedrock, (Map A, fig. 1; also see figs. 2, 3, 4, on sheet 8). Subparallel to divergent seismic reflections show that sediments onlap bedrock to the northeast and downlap folded sediments to the southwest. This wedge is inferred to consist primarily of relatively coarse-grained sediments (sheet 10) derived from local watersheds with the highest sediment accumulation rates occurring about 30,000 to 21,000 years ago when this zone occupied the nearshore during the last sea-level fall.

The second notable zone of increased sediment thickness (Map B on sheet 9) is about 2 km wide and parallels the short in the southeastern part of the map area at water depths of about 60 to 85 m. The inner, northeastern part of this zone contains a downlapping sediment wedge similar to that of the first zone (see figs. 9, 10 on sheet 8). The outer, southwestern part of this second zone occurs in an area of fine-grained surface sediments, a “mud belt” derived from the Russian River, which enters the Pacific

Ocean about 15 km southeast of the map area (Map B; Klise, 1984; Drake and Cacchione, 1985). The Russian River has a large sediment load (estimated 900,000 metric tons/yr; Farnsworth and Warrick, 2007) resulting in increased sediment thickness in this midshelf area.

Local coastal watersheds are significantly less important sediment sources. These watersheds extend just 2 to 3 km east from the shoreline and their role as sediment sources diminished during sea-level rise as the seaward portions of their drainage basins became submerged.

Five different "domains" of sediment thickness are recognized on the regional sediment-thickness map (Map D on sheet 9), each with distinctive geologic controls: (1) The Salt Point shelf domain, located in the far northwestern part of the region, has a mean sediment thickness of 11.7 m. The thickest sediment (20 to 25 m) is found where a pre-LGM, regressive, downlapping sediment wedge formed above a break in slope that is controlled by a contact between harder bedrock and softer, folded Pleistocene strata. Sediment thinning in this domain within the outer portions of California's State Waters is the result of a relative lack of sediment supply from local watersheds, as well as a more distal Russian River source. (2) The Russian River delta and mud belt domain, located offshore of the Russian River, the largest sediment source on this part of the coast, has the thickest uppermost Pleistocene and Holocene sediment in the region (mean thickness, 21.1 m). The northward extension of this domain into the midshelf "mud belt" results from northward shelf-bottom currents and sediment transport (Drake and Cacchione, 1985). This domain includes a section of the San Andreas Fault Zone, which here is characterized by several releasing, right-stepping strands that bound narrow, elongate pull-apart basins; these sedimentary basins contain the greatest thickness of uppermost Pleistocene and Holocene sediment (about 56 m) in the region. (3) The Bodega Head–Tomales Point shelf domain, located between Bodega Head and the Point Reyes headland, contains the least amount of sediment in the region (mean thickness, 3.4 m). The lack of sediment primarily results from decreased "accommodation space" (Catuneanu, 2006) and limited sediment supply. (4) The Point Reyes bar domain, located west and south of the Point Reyes headland, is a local zone of increased sediment thickness (mean thickness, 14.3 m) created by bar deposition on the more protected south flank of the Point Reyes headland during rising sea level. (5) The Bolinas shelf domain, located east and southeast of the Point Reyes headland, has a thin sediment cover (mean thickness, 5.6 m), which likely results from limited sediment accommodation space caused by tectonic uplift (water depths in this domain within California's State Waters are less than 45 m), and high wave energy, capable of reworking and transporting shelf sediment to deeper water.

Table 7–1. Area, uppermost Pleistocene and Holocene sediment-thickness, and sediment-volume data for California's State Waters in Salt Point to Drakes Bay region (domains 1–5), as well as in Offshore of Salt Point map area.

Regional sediment-thickness domains in Salt Point to Drakes Bay region			
	Area (km^2)	Mean sediment thickness (m)	Sediment volume ($10^6 m^3$)
Entire Salt Point to Drakes Bay region	714	9.5	6,794
(1) Salt Point shelf	90	11.7	1,054
(2) Russian River delta and mud belt	144	21.1	3,031
(3) Bodega Head–Tomales Point shelf	275	3.4	928
(4) Point Reyes bar	72	14.3	1,029
(5) Bolinas shelf	133	5.6	752
Sediment thickness in Offshore of Salt Point map area			
Offshore of Salt Point map area	101	12.1	1,226
Salt Point shelf	90	11.7	1,052
Russian River delta and mud belt	11	15.4	174

Chapter 8. Geologic and Geomorphic Map of the Offshore of Salt Point Map Area (Sheet 10)

By Samuel Y. Johnson, Stephen R. Hartwell, and Michael W. Manson

Geologic and Geomorphic Summary

Marine geology and geomorphology were mapped in the Offshore of Salt Point map area from approximate Mean High Water (MHW) to the 3-nautical-mile limit of California's State Waters. MHW is defined at an elevation of 1.46 m above the North American Vertical Datum of 1988 (NAVD 88) (Weber and others, 2005). Offshore geologic units (table 8-1) were delineated on the basis of integrated analyses of adjacent onshore geology with multibeam bathymetry and backscatter imagery (sheets 1, 2, 3), seafloor-sediment and rock samples (Reid and others, 2006), digital camera and video imagery (sheet 6), and high-resolution seismic-reflection profiles (sheet 8). Aerial photographs taken in multiple years were used to map the nearshore area (0 to 10 m water depth) and to link the offshore and onshore geology.

Onshore geologic mapping was compiled from Huffman (1972), California Geological Survey (1974), Blake and others (2002), Fuller and others (2002), and Manson and others (2006). Quaternary unit designations are adapted from Witter and others (2006).

The morphology and the geology of the Offshore of Salt Point map area result from the interplay between local sea-level rise, sedimentary processes, oceanography, and tectonics. The offshore part of the map area extends from the shoreline to water depths of about 90 to 100 m on the mid-continental shelf; the shelf break occurs about 20 km farther offshore at water depths of about 200 m. The nearshore to inner shelf area (to water depths of about 50 to 60 m) typically dips seaward about 1.0° to 1.5°; the mid to outer shelf area dips more gently, generally less than 0.5°. Sea level has risen about 125 to 130 m over about the last 21,000 years (for example, Lambeck and Chappell, 2001; Peltier and Fairbanks, 2006), leading to broadening of the continental shelf, progressive eastward migration of the shoreline and wave-cut platform, and associated transgressive erosion and deposition. Land-derived sediment was carried into this dynamic setting, and then subjected to full Pacific Ocean wave energy and strong currents before deposition or offshore transport. Tectonic influences on shelf morphology and geology include local faulting, folding, uplift, and subsidence.

Bedrock of the Paleocene and Eocene German Rancho Formation (unit Tgr) underlies much of the inner shelf, extending to water depths of as much as 60 m. Although onshore coastal outcrops of this unit are well bedded, seafloor outcrops imaged on high-resolution bathymetry (sheets 1, 2) have a hackly surface texture and abundant fractures. Embayments in the outer margin of the seafloor bedrock outcrops are commonly paired with the mouths of coastal watersheds and are inferred to have formed by fluvial erosion during the last sea-level lowstand. One of the more prominent embayments occurs about one kilometer north of Salt Point at the mouth of Miller Creek (fig. 1–2). These coastal watersheds are relatively small and steep, extending to a drainage divide just 2 to 3 km east of the shoreline, and are inferred sources of coarse-grained sediments. Immediately east of this onshore topographic divide, drainage along this part of the coast is captured by the northwest-flowing South Fork of the Gualala River (fig. 1–2), which runs parallel to the coast along the trace of the San Andreas Fault.

Given relatively shallow water depths (0 to about 50 m) and exposure to high wave energy, modern nearshore to midshelf sediments are mostly sand (unit Qms) and a mix of sand, gravel, and cobbles (units Qmsc and Qmsd). Coarser grained sands and gravels (units Qmsc and Qmsd) are recognized primarily on the basis of bathymetry and high backscatter (sheets 1, 2, 3). Both units Qmsc and Qmsd typically have abrupt landward contacts with bedrock (unit Tgr) and they form irregular to

lenticular exposures that are commonly elongate in the shore-normal direction. Contacts between units Qmsc and Qms typically are gradational.

Unit Qmsd typically is mapped as erosional lags in scour depressions (see, for example, Cacchione and others, 1984) that are bounded by relatively sharp or, less commonly, diffuse contacts with the horizontal sand sheets of unit Qms. These depressions typically are a few tens of centimeters deep and range in area from a few tens of square meters to more than one square kilometer. Such scour depressions are common along this stretch of the California coast (see, for example, Cacchione and others, 1984; Hallenbeck and others, 2012; Davis and others, 2013) where offshore sandy sediment can be relatively thin (thus unable to fill the depressions) owing to lack of sediment supply from rivers and also to significant erosion and offshore transport of sediment during large northwest winter swells. Such features have been referred to as "rippled-scour depressions" (see, for example, Cacchione and others, 1984) or "sorted bedforms" (see, for example, Murray and Thieler, 2004; Goff and others, 2005; Trembanis and Hume, 2011). Although the general areas in which both unit Qmsd scour depressions and surrounding Qms sand sheets are found are not likely to change substantially, the boundaries of the unit(s) likely are ephemeral, changing seasonally and during significant storm events.

The offshore decrease in slope at midshelf water depths (about 60 m) approximately coincides with a transition to finer grained marine sediments (unit Qmsf), which extends to the outer (3-nautical-mile) limit of California's State Waters. Unit Qmsf consists primarily of mud and muddy sand and is commonly extensively bioturbated. These fine-grained sediments are inferred to have been derived from the Russian River, the mouth of which is about 15 km south of the map area. Both Drake and Cacchione (1985) and Sherwood and others (1994) have documented seasonal, midshelf, northwest-directed, bottom currents capable of transporting fine-grained, suspended sediment from the Russian River to the Offshore of Salt Point map area.

The onshore part of the Offshore of Salt Point map area is cut by the northwest-striking San Andreas Fault, the right-lateral transform boundary between the North American and Pacific tectonic plates. The San Andreas Fault extends offshore about 5 km south of the map area near Fort Ross, and about 50 km north of the map area on the east flank of Point Arena. The onland, "north coast" section of the San Andreas Fault has an estimated slip rate of about 17 to 25 mm/yr (Bryant and Lundberg, 2002). The last ground rupture in the map area (Brown and Wolfe, 1972) occurred during the devastating great 1906 California earthquake (M7.8, 4/18/1906), thought to have nucleated on the San Andreas Fault about 100 kilometers to the south offshore of San Francisco (for example, Bolt, 1968; Lomax, 2005). Emergent marine terraces along the coast in the Offshore of Salt Point map area record recent contractional deformation associated with the San Andreas Fault Zone. Prentice and Kelson (2006) reported uplift rates of 0.3 to 0.6 mm/yr for a nearby late Pleistocene terrace (exposed at Fort Ross, about 5 km south of the map area), which must have affected the nearshore and inner shelf.

The coast between Fort Ross and Point Arena, the northwesternmost exposed section west of the San Andreas Fault, is known as the "Gualala Block" (fig. 1–1) on the basis of its distinctive geology, which has been widely used to develop paleogeographic reconstructions of coastal California that restore as much as 150 to 180 km of right-lateral slip on the combined San Andreas and San Gregorio Fault systems (see, for example, Wentworth, 1968; Wentworth and others, 1998; Jachens and others, 1998; Dickinson and others, 2005; Burnham, 2009). The Gualala Block is underlain by a thick (as much as 9 to 11 km, in aggregate), discontinuous Upper Cretaceous to Miocene stratigraphic section (summarized in Wentworth and others, 1998), however only the Paleocene and Eocene German Rancho Formation (unit Tgr) is exposed onshore and is inferred to form seafloor bedrock outcrops in the Offshore of Salt Point map area. The German Rancho Formation consists of sandstone, mudstone, and conglomerate interpreted as deep-water, submarine-fan deposits.

The western boundary of the Gualala Block is located offshore. Using seismic-reflection data, McCulloch (1987; his fig. 14) mapped a shore-parallel fault about 3 to 5 km offshore, which Dickinson

and others (2005) subsequently named the Gualala Fault. Jachens and others (1998) evaluated aeromagnetic and gravity data across this zone and modeled this structure as a steep fault within the Salinian basement block, characterized by 3 to 5 km of right-lateral offset. In contrast, Dickinson and others (2005) consider the Gualala Fault a late Miocene strand of the San Andreas Fault, separating Salinian and Franciscan basement rocks, with minimum right-lateral slip of 70 km. Our analysis of deeper industry seismic-reflection data within California's State Waters shows the Gualala Fault as a steep, northeast-dipping structure (figs. 5, 8 on sheet 8). Shallower seismic-reflections crossing the Gualala Fault reveal a thick late(?) Pleistocene section characterized by recent faulting and gentle asymmetric folding (figs. 1, 2, 3, 4, 6, 7, 9, 10 on sheet 8). Hence, the Gualala Fault appears to be a recently active "blind" structure that has deformed young sediments. Our mapping also documents a more nearshore zone of deformation that we refer to as the "east Gualala deformation zone." This zone extends through the central and southern parts of the Offshore of Salt Point map area and is similarly characterized by steep faults and gentle folds that deform inferred late Pleistocene strata.

Table 8–1. Areas and relative proportions of offshore geologic map units in Offshore of Salt Point map area.

Map Unit	Area (m^2)	Area (km^2)	Percent of total area
Marine sedimentary units			
Qms	12,290,277	12.3	9.7
Qmsc	3,142,139	3.1	2.5
Qmsf	94,046,427	94.0	74.0
Qmsd	4,563,626	4.6	3.6
Total sedimentary units	14,042,468	114.0	89.7
Marine bedrock and (or) shallow bedrock units			
Tgr	13,030,254	13.0	10.3
Total bedrock units	13,030,254	13.0	10.3
Total Offshore of Salt Point map area	127,072,722	127.1	100.0

DESCRIPTION OF MAP UNITS

OFFSHORE GEOLOGIC AND GEOMORPHIC UNITS

Qms **Marine nearshore and shelf deposits (late Holocene)—**Mostly sand (some mud); ripple marks common; found on gently seaward-dipping (less than 2°) surface that extends from shoreline to water depths of about 60 m

Qmsc **Coarse-grained marine nearshore and shelf deposits (late Holocene)—**Predominantly coarse sand, gravel, and cobbles; found on gently seaward-dipping (less than 2°) surface in water depths typically less than about 60 m; recognized primarily on basis of high backscatter and flat relief. Mapped occurrences are generally in contact with and occur seaward of unit Tgr bedrock

Qmsf **Fine-grained marine shelf deposits (late Holocene)**—Predominantly mud, very fine sand, and silt; commonly bioturbated; found on gently seaward-dipping (less than 0.5°) surface at depths greater than about 50 to 60 m

Qmsd **Marine shelf scour depressions (late Holocene)—**Inferred to be coarse sand and possibly gravel; consists of irregular, arcuate scour depressions that vary from solitary features occupying a few hundred square meters to fields of interconnected depressions covering tens of thousands of square meters. Found as single depressions or in fields of depressions interspersed with elevated shelf sediments (units Qms and Qmsc), and are typically in contact with and occur seaward of unit Tgr bedrock. Depressions typically are 15 to 50 cm deep, and they have sharp to diffuse boundaries. In map area, both backscatter data and direct camera observations (sheets 3 and 6, this report) show small intensity contrasts, suggesting that depressions are filled with sediment that is coarser than intervening elevated sandy shelf deposits; general area in which unit is found is not likely to change substantially, but boundaries of unit(s) and locations of individual depressions (and intervening flat sheets) likely are ephemeral, changing during significant storm events

Tgr **German Rancho Formation (Elder, 1998) (Eocene and Paleocene)**—Well-bedded, fine- to medium-grained sandstone, mudstone and conglomerate

ONSHORE GEOLOGIC AND GEOMORPHIC UNITS

[Bedrock units are compiled from Huffman (1972), California Geological Survey (1974), Blake and others (2002), Fuller and others (2002), and Manson and others (2006). Quaternary unit designations are from Witter and others (2006)]

af **Artificial fill (late Holocene)**—Material placed by humans

Qsc **Stream channel deposits (late Holocene)**—Fluvial deposits within active, natural stream channels

Qt **Stream terrace deposits (late Holocene)**—Stream terrace deposits judged to be latest Holocene (<1,000 years) in age based on records of historical inundation, the identification of youthful meander scars and braid bars on aerial photographs and (or) lidar images

Qot **Stream terrace deposits (Holocene)**—Stream terrace deposits that were deposited in point bar and overbank settings

Qf **Alluvial fan deposits (Holocene)**—Sediment deposited by streams emanating from mountain canyons onto alluvial valley floors or alluvial plains; may include debris flow, hyper-concentrated mudflow, and braided stream deposits

Qls **Landslide deposits (Holocene and Pleistocene)**—Weathered and disintegrated rocks and soil, mapped units range from deep-seated landslides to active colluvium. Internal contacts differentiate individual landslide bodies

Qmt **Marine-terrace deposits (late Pleistocene)**—Sand, gravel, and cobbles; deposited on marine-abrasion platforms and later uplifted to present-day elevations along coast

Tor **Ohlson Ranch Formation (Blake and others, 2002) (Pliocene)**—Horizontal, thickly bedded, well-consolidated sandstone

Tgr **German Rancho Formation (Elder, 1998) (Eocene and Paleocene)**—Well-bedded, fine- to medium-grained sandstone, mudstone and conglomerate (Wentworth and others, 1998)

TKu **German Rancho Formation and Gualala Formation (Elder, 1998), undivided (Eocene, Paleocene, and Late Cretaceous)**—sandstone, conglomerate, mudstone, and shale

Franciscan complex

TKfss **Sandstone within the Coastal Belt (late Eocene to Late Cretaceous)**—Mostly massive, feldspathic and feldspathic-lithic wacke; overlies Late Cretaceous to middle Eocene basalt and pelagic limestone (Bachman, 1978; Sliter, 1984; Blake and others, 2002)

TKfs **Sandstone within the Coastal or Central Belts (late Eocene to Late Cretaceous)**—Mostly massive, feldspathic-lithic wacke, lacks known fossils or other stratigraphic control (Blake and others, 2002)

KJfs **Graywacke and mélange within the Central Belt (Cretaceous and Jurassic)**—Massive to well-bedded lithic wacke, siltstone, shale, and slate, grading into mélange consisting of sheared argillite and graywacke matrix enclosing blocks and lenses of sedimentary, metamorphic, and volcanic rocks

sp **Serpentinite blocks and lenses within the mélange of the Central Belt (Cretaceous and(or) Jurassic)**

Acknowledgments

This publication was funded by the California Ocean Protection Council and the U.S. Geological Survey (USGS) Coastal and Marine Geology Program. We thank the officers, crew, and scientific parties of the ships—R/V VenTresca, California State University, Monterey Bay, Seafloor Mapping Lab; and F/V Quicksilver, Fugro Pelagos—for their skill and professionalism in collecting the data presented in this report. We thank Katherine Maier Coble, Stephen Watt, and Scott Starratt (all USGS) for their critical reviews that greatly improved this report. We are very grateful to USGS editor Taryn Lindquist for helping us develop the templates and formats for this series of publications, and for invaluable editorial review and suggestions.

References Cited

Anderson, T.B., 1998, Turbidite sequences in the German Rancho Formation (Paleocene-Eocene), northwest Sonoma County coastline, California, *in* Elder, W.P., ed., Geology and tectonics of the Gualala block, northern California: Pacific Section, Society of Economic Paleontologists and Mineralogists, Book 84, p. 137–148.

Anderson, T.J., Cochrane, G.R., Roberts, D.A., Chezar, H., and Hatcher, G., 2007, A rapid method to characterize seabed habitats and associated macro-organisms, *in* Todd, B.J., and Greene, H.G., eds., Mapping the seafloor for habitat characterization: Geological Association of Canada Special Paper 47, p. 71–79.

Bachman, S.B., 1978, A Cretaceous and early Tertiary subduction complex, Mendocino coast, northern California: Los Angeles, Pacific Section Society of Economic Paleontologists and Mineralogists, Pacific Coast Paleogeography Symposium, no. 2, p. 419–43.

Blake, M.C., Jr., Graymer, R.W., and Stamski, R.E., 2002, Geologic map and map database of western Sonoma, northernmost Marin, and southernmost Mendocino counties, California: U.S. Geological Survey Miscellaneous Field Studies Map 2402, scale 1:100,000, available at http://pubs.usgs.gov/mf/2002/2402/.

Bolt, B.A., 1968, The focus of the 1906 California earthquake: Bulletin of the Seismological Society of America, v. 58, p. 457–471.

Brown, R.D., Jr., and Wolfe, E.W., 1972, Map showing recently active breaks along the San Andreas Fault between Point Delgada and Bolinas Bay, California: U.S. Geological Survey Miscellaneous Investigations Map I-692, scale 1:24,000.

Bryant, W.A., and Lundberg, M.M., compilers, 2002, Fault number 1b, San Andreas fault zone, North Coast section, *in* Quaternary fault and fold database of the United States: U.S. Geological Survey website, accessed April 4, 2013, at http://earthquakes.usgs.gov/hazards/qfaults/.

Burnham, K., 2009, Predictive model of San Andreas Fault system paleogeography, Late Cretaceous to early Miocene, derived from detailed multidisciplinary conglomerate correlations: Tectonophysics 464, p. 195–258, doi:10.1016/j.tecto.2007.11.056.

Cacchione, D.A., Drake, D.E., Grant, W.D., and Tate, G.B., 1984, Rippled scour depressions on the inner continental shelf off central California: Journal of Sedimentary Petrology, v. 54, p. 1,280–1,291.

California Department of Fish and Wildlife, 2008, California Marine Life Protection Act master plan for marine protected areas—Revised draft: California Department of Fish and Wildlife [formerly California Department of Fish and Game], available at http://www.dfg.ca.gov/mlpa/masterplan.asp.

California Department of Fish and Wildlife, 2012, Guide to the North-Central California Marine Protected Areas, Point Arena to Pigeon Point: 67 p., accessed May 1, 2013, at http://www.dfg.ca.gov/marine/mpa/nccmpas_list.asp.

California Geological Survey, 1974, Alquist-Priolo Earthquake Fault Zone Maps of Annapolis and Plantation quadrangles, scale 1:24,000, available at http://www.quake.ca.gov/gmaps/WH/regulatorymaps.mtm.

Cass, A.J., Beamish, R.J., and McFarlane, G.A., 1990, Lingcod (*Ophiodon elongatus*): Canadian Journal of Fisheries and Aquatic Sciences, Special Publication 109, 40 p.

Catuneanu, O., 2006, Principles of sequence stratigraphy: Amsterdam, Elsevier, 375 p.

Cochrane, G.R., 2008, Video-supervised classification of sonar data for mapping seafloor habitat, *in* Reynolds, J.R., and Greene, H.G., eds., Marine habitat mapping technology for Alaska: Fairbanks, University of Alaska, Alaska Sea Grant College Program, p. 185–194, available at http://doc.nprb.org/web/research/research%20pubs/615_habitat_mapping_workshop/Individual%20Chapters%20High-Res/Ch13%20Cochrane.pdf.

Cochrane, G.R., Conrad, J.E., Reid, J.A., Fangman, S., and Golden, N., 2005, Nearshore benthic habitat GIS for the Channel Islands National Marine Sanctuary and southern California state fisheries reserves, vol. II: U.S. Geological Survey Open-File Report 2005–1170, available at http://pubs.usgs.gov/of/2005/1170/.

Cochrane, G.R., Nasby, N.M., Reid, J.A., Waltenberger, B., and Lee, K.M., 2003, Nearshore benthic habitat GIS for the Channel Islands National Marine Sanctuary and southern California state fisheries reserves, vol. 1: U.S. Geological Survey Open-File Report 03–85, available at http://pubs.usgs.gov/of/2003/0085/.

Davis, A.C.D., Kvitek, R.G., Mueller, C.B.A., Young, M.A., Storlazzi, C.D., and Phillips, E.L., 2013, Distribution and abundance of rippled scour depressions along the California coast: Continental Shelf Research, v. 69, p. 88–100, doi:10.1016/j.csr.2013.09.010.

Dickinson, W.R., Ducea, M., Rosenberg, L.I., Greene, H.G., Graham, S.A., Clark, J.C., Weber, G.E., Kidder, S., Ernst, W.G., and Brabb, E.E., 2005, Net dextral slip, Neogene San Gregorio–Hosgri fault zone, coastal California—Geologic evidence and tectonic implications: Geological Society of America Special Paper 391, 43 p, doi:10.1130/2005.2391.

Drake, D.E., and Cacchione, D.A., 1985, Seasonal variation in sediment transport on the Russian River shelf, California: Continental Shelf Research, v. 4, p. 495–514, doi:10.1016/0278-4343(85)90007-X.

Elder, W.P., ed., 1998, Geology and tectonics of the Gualala Block, northern California: Pacific Section, Society of Economic Paleontologists and Mineralogists, Book 84, 222 p.

Fader, G.B.J., 1997, Effects of shallow gas on seismic-reflection profiles, *in* Davies, T.A., Bell, T., Cooper, A.K., Josenhans, H., Polyak, L., Solheim, A., Stoker, M.S., and Stravers, J.A., eds., Glaciated continental margins—An atlas of acoustic images: London, Chapman & Hall, p. 29–30.

Fairbanks, R.G., 1989, A 17,000-year glacio-eustatic sea level record—Influence of glacial melting rates on the Younger Dryas event and deep-ocean circulation: Science, v. 342, p. 637–642.

Farnsworth, K. L., and Warrick, J.A., 2007, Sources, dispersal, and fate of fine sediment supplied to coastal California: U.S. Geological Survey Scientific Investigations Report 2007–5254, 77 p., available at http://pubs.usgs.gov/sir/2007/5254/.

Fleming, K., Johnston, P., Zwartz, D., Yokoyama, Y., Lambeck, K., and Chappell, J., 1998, Refining the eustatic sea-level curve since the Last Glacial Maximum using far- and intermediate-field sites: Earth and Planetary Science Letters, v. 163, p. 327–342, doi:10.1016/S0012-821X(98)00198-8.

Fuller, M.S., Haydon, W.D., Purcell, M.G., and Custis, K., 2002, Geologic and geomorphic features related to landsliding, Gualala River watershed, Sonoma and Mendocino counties, California: California Geological Survey Watershed Mapping Series, Map Set 5, Plate 1, Sheet 3 of 3, scale 1:24,000, available at http://www.conservation.ca.gov/cgs/fwgp/Pages/gualala.aspx.

Goff, J.A., Mayer, L.A., Traykovski, P., Buynevich, I., Wilkens, R., Raymond, R., Glang, G., Evans, R.L., Olson, H., and Jenkins, C., 2005, Detailed investigations of sorted bedforms, or "rippled scour depressions," within the Martha's Vineyard Coastal Observatory, Massachusetts: Continental Shelf Research, v. 25, p. 461–484, doi:10.1016/j.csr.2004.09.019.

Greene, H.G., Bizzarro, J.J., O'Connell, V.M., and Brylinsky, C.K., 2007, Construction of digital potential marine benthic habitat maps using a coded classification scheme and its application, *in* Todd, B.J., and Greene, H.G., eds., Mapping the seafloor for habitat characterization: Geological Association of Canada Special Paper 47, p. 141–155.

Greene, H.G., Bizzarro, J.J., Tilden, J.E., Lopez, H.L., and Erdey, M.D., 2005, The benefits and pitfalls of geographic information systems in marine benthic habitat mapping, *in* Wright, D.J., and Scholz, A.J., eds., Place matters: Portland, Oregon State University Press, p. 34–46.

Greene, H.G., Yoklavich, M.M., Starr, R.M., O'Connell, V.M., Wakefield, W.W., Sullivan, D.E., McRea, J.E., and Cailliet, G.M., 1999, A classification scheme for deep seafloor habitats: Oceanologica Acta, v. 22, p. 663–678.

Hallenbeck, T.R., Kvitek, R.G., and Lindholm, J., 2012, Rippled scour depressions add ecologically significant heterogeneity to soft-bottom habitats on the continental shelf: Marine Ecology Progress Series, v. 468, p. 119–133, doi:10.3354/meps09948.
Heck, R.G., Edwards, E.B., Kronen, J.D., Jr., and Willingham, C.R., 1990, Petroleum potential of the offshore outer Santa Cruz and Bodega basins, California, *in* Garrison, R.E., Greene, H.G., Hicks, K.R., Weber, G.E., and Wright, T.L., eds. Geology and tectonics of the central California coastal region, San Francisco to Monterey: American Association of Petroleum Geologists, Pacific Section, Bulletin GB67, p. 143–164.
Hickey, B.M., 1979, The California current system—Hypotheses and facts: Progress in Oceanography, v. 8, p. 191–279.
Hovland, M., and Judd, A.G., 1988, Seabed pockmark and seepages—Impact on geology, biology and the marine environment: London, Graham and Trotman, Inc., 293 p.
Huffman, M.E., 1972, Geology for planning on the Sonoma County coast between the Russian and Gualala Rivers: California Division of Mines and Geology Preliminary Report 16, 38 p., 4 plates, scale 1:24,000.
Jachens, R.C., Wentworth, C.M., and McLaughlin, R.J., 1998, Pre-San Andreas location of the Gualala Block inferred from magnetic and gravity anomalies, *in* Elder, W.P., ed., Geology and tectonics of the Gualala block, northern California: Pacific Section, Society of Economic Paleontologists and Mineralogists, Book 84, p. 27–53.
Klise, D.H., 1984, Modern sedimentation on the California continental margin adjacent to the Russian River: M.S. thesis, San Jose State University, 120 p.
Kvitek, R., Bretz, C., Cochrane, G.R., and Greene, H.G., 2006, Final report, Statewide Marine Mapping Planning Workshop, December 12–13, 2005, Seaside, Calif.: California State University, Monterey Bay, 108 p., available at http://euclase.csumb.edu/DATA_DOWNLOAD/StrategicMapgWrkshp05/MappingWorkshop12_12-13/Final_Report/CA%20Habitat%20Mapping%20Rpt.pdf.
Lambeck, K., and Chappell, J., 2001, Sea level change through the last glacial cycle: Science, v. 292, p. 679–686, doi:10.1126/science.1059549.
Lawson, A.C., ed., 1908, The California earthquake of April 18, 1906, Report of the State Earthquake Investigation Commission: Carnegie Institution of Washington Publication 87, v. 1, 1451 p. and atlas.
Lomax, A., 2005, A reanalysis of the hypocentral location and related observations for the Great 1906 California earthquake: Bulletin of the Seismological Society of America, v. 95, p. 861–877, doi:10.1785/0120040141.
Love, M.S., Yoklavich, M., Thorsteinson, L., and Butler, J., 2002, The rockfishes of the northeast Pacific: Berkeley, University of California Press, 405 p., doi:10.5860/CHOICE.40-3403.
Madden, C.J., Goodin, K.L., Allee, R., Finkbeiner, M., and Bamford, D.E., 2008, Draft Coastal and Marine Ecological Classification Standard: National Oceanic and Atmospheric Administration (NOAA) and NatureServe, v. III, 77 p.
Manson, M.W., Huyette, C.M., Wills, C.J., Huffman, M.E., Smelser, G.G., Fuller, M.E., Domrose, C., and Gutierrez, C., 2006, Landslides in the Highway 1 corridor between Bodega Bay and Fort Ross, Sonoma County, California: California Geological Survey Special Report 196, 26 p., 2 plates, 38 maps, scale 1:12,000.
McCulloch, D.S., 1987, Regional geology and hydrocarbon potential of offshore Central California, *in* Scholl, D.W., Grantz, A., and Vedder, J.G., eds., Geology and resource potential of the continental margin of western North America and adjacent ocean basins—Beaufort Sea to Baja California: Circum-Pacific Council for Energy and Mineral Resources, Earth Science Series, v. 6, p. 353–401.
Mitchum, R.M., Jr., Vail, P.R., and Sangree, J.B., 1977, Seismic stratigraphy and global changes of sea level, part 6—Stratigraphic interpretation of seismic reflection patterns in depositional sequences, *in*

Payton, C.E., ed., Seismic stratigraphy—Applications to hydrocarbon exploration: Tulsa, Okla., American Association of Petroleum Geologists, p. 117–133.
Murray, B., and Thieler, E.R., 2004, A new hypothesis and exploratory model for the formation of large-scale inner-shelf sediment sorting and “rippled scour depressions”: Continental Shelf Research, v. 24, no. 3, p. 295–315, doi:10.1016/j.csr.2003.11.001.
Northern California Earthquake Data Center, 2014, Northern California earthquake catalog: Northern California Earthquake Data Center database, accessed April 5, 2014, at http://www.ncedc.org/ncsn/.
Peltier, W.R., and Fairbanks, R.G., 2006, Global glacial ice volume and Last Glacial Maximum duration from an extended Barbados sea level record: Quaternary Science Reviews, v. 25, p. 3,322–3,337, doi:10.1016/j.quascirev.2006.04.010.
Phillips, E.L., Storlazzi, C.D., Dartnell, P. and Edwards, B.D., 2007, Exploring rippled scour depressions offshore Huntington Beach, California: Coastal Sediments 2007, v. 3, p. 1,851–1,864.
Petersen, M.D., Frankel, A.D., Harmsen, S.C., Mueller, C.S., Haller, K.M., Wheeler, R.L., Wesson, R.L., Zeng, Y., Boyd, O.S., Perkins, D.M., Luco, N., Field, E.H., Wills, C.J., and Rukstales, K.S., 2008, Documentation for the 2008 update of the United States National Seismic Hazard Maps: U.S. Geological Survey Open-File Report 2008–1128, 61 p., available at http://pubs.usgs.gov/of/2008/1128/.
Prentice, C.S., and Kelson, K.I., 2006, The San Andreas fault in Sonoma and Mendocino counties, *in* Prentice, C.S., Scotchmoor, J.G., Moores, E.M., and Kiland, J.P., eds., 1906 San Francisco Earthquake Centennial Field Guides: Field trips associated with the 100th Anniversary Conference, 18–23 April 2006, San Francisco, California: Geological Society of America Field Guide 7, p. 127–156, doi:10.1130/2006.1906SF(11).
Reid, J.A., Reid, J.M., Jenkins, C.J., Zimmerman, M., Williams, S.J., and Field, M.E., 2006, usSEABED—Pacific Coast (California, Oregon, Washington) offshore surficial-sediment data release: U.S. Geological Survey Data Series 182, available at http://pubs.usgs.gov/ds/2006/182/.
Sherwood, C.R., Butman, B., Cacchione, D.A., Drake, D.E., Gross, T.F., Sternberg, R.W., Wiberg, P.L., and Williams, A.J., III, 1994, Sediment transport events on the northern California continental shelf during the 1990–1991 STRESS experiment: Continental Shelf Research, v. 14, p. 1063–1099, doi:10.1016/0278-4343(94)90029-9.
Sliter, W.V., 1984, Foraminifers from Cretaceous limestone of the Franciscan Complex, northern California, *in* Blake, M.C., Jr., ed., Franciscan Geology of Northern California: Pacific Section, Society of Economic Paleontologists and Mineralogists, v. 43, p. 149–162.
Stanford, J.D., Hemingway, R., Rohling, E.J., Challenor, P.G., Medina-Elizalde, M., and Lester, A.J., 2011, Sea-level probability for the last deglaciation—A statistical analysis of far-field records: Global and Planetary Change, v. 79, p. 193–203, doi:10.1016/j.gloplacha.2010.11.002.
Storlazzi, C.D., and Griggs, G.B., 2000, Influence of El Nino-Southern Oscillation (ENSO) events on the evolution of central California’s shoreline: Geological Society of America Bulletin, v. 112, p. 236–249.
Storlazzi, C.D., and Wingfield, D.K., 2005, Spatial and temporal variations in oceanographic and meteorologic forcing along the central California coast, 1980-2002: U.S. Geological Survey Scientific Investigations Report 2005–5085, 39 p., available at http://pubs.usgs.gov/sir/2005/5085/.
Tissot, B.N., Yoklavich, M.M., Love, M.S., York, K., and Amend, M., 2006, Benthic invertebrates that form habitat on deep banks off southern California, with special reference to deep sea coral: Fishery Bulletin, v. 104, p. 167–181.
Trembanis, A.C., and Hume, T.M., 2011, Sorted bedforms on the inner shelf off northeastern New Zealand—Spatiotemporal relationships and potential paleo-environmental implications: Geo-Marine Letters, v. 31, p. 203–214, doi:10.1007/s00367-010-0225-8.

U.S. Geological Survey, 2009, National Archive of Marine Seismic Surveys: U.S. Geological Survey database, available at http://walrus.wr.usgs.gov/NAMSS/.
U.S. Geological Survey and California Geological Survey, 2010, Quaternary fault and fold database of the United States: U.S. Geological Survey database, accessed April 5, 2014, at http://earthquake.usgs.gov/hazards/qfaults/.
Waelbroeck, C., Labeyrie, L., Michel, E., Duplessy, J.C., McManus, J.F., Lambeck, K., Balbon, E., and Labracherie, M., 2002, Sea-level and deep water temperature changes derived from benthic foraminifera isotopic records: Quaternary Science Reviews, v. 21, p. 295–305.
Weber, K.M., List, J.H., and Morgan, K.L., 2005, An operational Mean High Water datum for determination of shoreline position from topographic lidar data: U.S. Geological Survey Open-File Report 2005–1027, available at http://pubs.usgs.gov/of/2005/1027/.
Wentworth, C.K., 1922, A scale of grade and class terms for clastic sediments: Journal of Geology, v. 30, p. 377–392.
Wentworth, C.M., 1968, Upper Cretaceous and lower Tertiary strata near Gualala, California, and inferred large right slip on the San Andreas fault, *in* Dickinson, W.R., and Grantz, A., eds. Proceedings of conference on geologic problems of San Andreas fault system: Stanford University Publications, Geological Sciences, v. 11, p. 130–143.
Wentworth, C.M., Jones, D.L., and Brabb, E.E., 1998, Geology and regional correlation of the Cretaceous and Paleogene rocks of the Gualala block, California, *in* Elder, W.P., ed., Geology and tectonics of the Gualala block, northern California: Pacific Section, Society of Economic Paleontologists and Mineralogists, Book 84, p. 3–26.
Witter, R.C., Knudsen, K.L., Sowers, J.M., Wentworth, C.M., Koehler, R.D., Randolph, C.E., Brooks, S.K., and Gans, K.D., 2006, Maps of Quaternary deposits and liquefaction susceptibility in the central San Francisco Bay region, California: U.S. Geological Survey Open-File Report 2006–1037, scale 1:24,000, available at http://pubs.usgs.gov/of/2006/1037/.
Wong, F.L., Phillips, E.L., Johnson, S.Y, and Sliter, R.W., 2012, Modeling of depth to base of Last Glacial Maximum and seafloor sediment thickness for the California State Waters Map Series, eastern Santa Barbara Channel, California: U.S. Geological Survey Open-File Report 2012–1161, 16 p., available at http://pubs.usgs.gov/of/2012/1161/.
Wright, D.J., Pendleton, M., Boulware, J., Walbridge, S., Gerlt, B., Eslinger, D., Sampson, D., and Huntley, E., 2012, ArcGIS Benthic Terrain Modeler (BTM), v. 3.0: Environmental Systems Research Institute and NOAA Coastal Services Center, Massachusetts Office of Coastal Zone Management, accessed February 1, 2014, at http://esriurl.com/5754.